Analytic properties and accuracy of the generalized Blackman-Esterling-Berk coherent-potential approximation

Klaus Koepernik
MPI ''Physics of Complex Systems,'' D-01887 Dresden, Germany

B. Velický
Charles University, Prague, Czech Republic

Roland Hayn and Helmut Eschrig
MPG Research Group Electron Systems, Department of Physics, TU Dresden D-01062, Dresden, Germany

(Received 1 September 1997)

The Blackman-Esterling-Berk (BEB) theory, generalized to nonorthogonal basis sets and complicated elementary cells [K. Koepernik, B. Velický, R. Hayn, and H. Eschrig, Phys. Rev. B **55**, 5717 (1997)], is inspected in great detail with respect to its analytic properties and numerical accuracy. We give a proof of the single impurity limit fulfilled by BEB theory, thus clarifying some critical points in the derivation of the theory. We undertake extensive numerical tests for the BEB coherent-potential approximation (CPA) to check the range of applicability of the included single-site approximation. The BEB CPA turns out to give good results in a wide range of energy parameters.
[S0163-1829(98)03228-7]

I. INTRODUCTION

This paper is devoted to the once famous BEB theory by Blackman, Esterling, and Berk[2] extending the use of the orbital coherent-potential approximation (CPA) to random off-diagonal matrix elements of the Hamiltonian (*off-diagonal disorder*). Our interest in this problem grew naturally out of our recent work on a first-principles charge self-consistent theory of the electronic structure of disordered alloys based on the CPA in a linear-combination of atomic orbitals (LCAO) representation.[1] We will refer to this paper as Ref. I. One of the conclusions of Ref. I was that the BEB CPA, after proper straightforward generalization, represents the natural formalism associated with the orbital CPA. Furthermore, its practical implementation led to results comparing very favorably with those obtained using techniques that represent the contemporary standard for the computation of electronic structures of random alloys, notably, the Korringa-Kohn-Rostocker (KKR) CPA, linear muffin-tin orbitals (LMTO) CPA, and LMTO tight-binding (TB) CPA; see Ref. 3 as a recent general reference for these methods. In fact, the structure of the BEB CPA parallels rather closely the Korringa-Kohn-Rostoker (KKR) CPA, but is free of the technical difficulties the KKR CPA faces when applied to complex structures.

All the foregoing suggests that BEB theory deserves attention on its own and should be revisited. This paper is then intended as a relatively independent complement to Ref. I, serving as a summary and an update of the general properties of BEB theory with several additions and clarifications. Our approach is both motivated and guided by the revived potential usefulness of the BEB method.

The BEB theory was announced in Ref. 2 in 1971, that is, in times prior to the KKR CPA, when the random alloy theory was still dominated by parameterized tight-binding Hamiltonians. It represented a major advance in comparison with the original TB CPA, which was suited only for the *site-diagonal disorder*, that is with only the site-diagonal elements of an orbital representation of the Hamiltonian allowed to vary stochastically according to the atomic species occupying the given site. Random off-diagonal elements (''hopping integrals'') clearly depend on both terminal points, and so they are seemingly beyond the reach of the so-called *single-site approximations*, as represented by the CPA. The ingenious BEB transformation is described particularly clearly in Ref. 4. It consisted in doubling the Hilbert space (for a binary alloy) by adding the atomic sort to the matrix indices. The off-diagonal part of the extended Hamiltonian became thus nonrandom, while the randomness on the site diagonal was represented by a random pseudospin variable indicating the actual random occupation of the site in question. A single-site approximation in the extended space yielded the BEB-CPA condition. There was a flurry of nearly simultaneously introduced alternative models with off-diagonal disorder, notably, the Shiba multiplicative model[5] with $t_{AB}^2 = t_{AA} t_{BB}$, t denoting the nearest-neighbor hopping integral. This model assumption led to a similarity transformation reducing the Shiba case to the diagonal disorder, at least as far as the site diagonal quantities, like self-energy and local projected densities of states were concerned. The Shiba assumption was appealing both physically and formally, by simplicity of the equations, and so it soon overshadowed the BEB approach; in particular, when it became clear that the Shiba approach is a special case of BEB (Ref. 6) and the latter seemed to be but a pointless mild generalization of the former, Ref. 7, p. 128. Soon thereafter, the whole TB or orbital approach fell out of fashion, and the advances were rather sporadic. Still, a number of features of BEB were analyzed, as is summarized in Ref. 19, Chap. X B.

A substantial deal of the results on BEB has been ob-

tained by its authors. Thus, the separated-band limit ($t_{AB}=0$) is already given in Ref. 2 as well as the proof that the first three moments of the spectral density and four of the total densities of states are reproduced by BEB exactly. The multiple-scattering approach was used in Ref. 4. The Shiba limit, of course, including also the diagonal CPA limit, was obtained in Ref. 6. Much of the later work centered around Gonis: in Ref. 8, the single-band case was treated, using several formalisms, including locators, propagators, and a variational technique. Most notably, a proof is given that the BEB CPA guarantees that the approximate Green's function is Herglotz, i.e., analytic in the upper half-plane of complex energies, with a negative-definite anti-Hermitian part. In Ref. 9, the first attempt to apply the BEB approximation to a realistic multiband case can be found. The results were promising, but not entirely convincing.

Other open points remained concerning BEB. Thus, the locator formalism, although natural in this case, required accepting ill-defined intermediate mathematical steps such as inversions of singular matrices.[4] There was the claim that the BEB CPA fails in the limit of dilute alloy,[5] which was just casually denied,[6] but never disproved. Another problem has been the supposedly small number of exact moments of the spectral density discussed above. Finally, the BEB theory works not only with an extended Hamiltonian matrix $H_{QQ'}$ but also with a Green's function matrix $G_{QQ'}$ with the same structure, whose elements are component projected doubly conditional averages of the alloy resolvent. Throughout the history of the BEB theory, starting from Ref. 2, Appendix D and ending with the recent review,[19] p. 241, this matrix was considered unphysical, and attempts were made to introduce the sum $\Sigma G_{QQ'}$ and a corresponding one-component effective coherent potential. In fact, however, the matrix structures like $G_{QQ'}$ represent the physical elements both in the KKR CPA and in the orbital CPA. This was recognized in another context already in the early eighties.[10] In Ref. I, this aspect of the orbital theory was linked directly to BEB theory, as will be discussed in Sec. II.

This paper has the following structure: In Sec. II, we paraphrase the main points of Ref. I relevant to the problem of the off-diagonal disorder and BEB. Section II A discusses the relation between the charge density, the orbitals, and the one-electron potential in real space, on the one hand, and the algebraic structure of the random matrices representing the alloy and subjected to the averaging procedures, on the other. It is shown how the basic features of the random Hamiltonian matrix lead in a nearly unique way to the generalized BEB representation of the alloy problem. Section II B serves to summarize the essential equations of the generalized BEB formalism, including the pseudospin notation in the extended space and the scattering formulation of the BEB-CPA self-consistency condition. Section III is dedicated to the general properties of the generalized BEB theory: in III A,we briefly characterize the BEB Green's function as a function of the complex energy variable, including the analytic properties and the spectral bounds. Then, the BEB CPA is presented as an interpolation scheme, including the limits of weak scattering and separate bands and the dilute limit. This limit of a vanishing concentration of one component is executed in detail, and the result is identified with the single impurity result, which can be derived directly (Sec. III B). A similar problem arises in the case of an alloy with a partial long-range order if some of the sublattices tend to be occupied by a single species. This case, first treated in Appendix A of Ref. I, is discussed in Sec. III C. Finally, in Sec. III D, we contrast the BEB approach to other descriptions of the off-diagonal disorder. The last section, IV, supplements the results obtainable analytically by a numerical analysis and serves to deal with several selected questions. We chose to study the simplest single-band case in one dimension because it is easily treated both by the CPA and by a direct simulation and because it is known to be extremely sensitive to the approximation of the CPA, i.e., mean-field type. On the whole, the BEB CPA is shown to be very flexible and to faithfully reproduce the salient features of the spectra found by direct simulation. This contrasts with other approaches tested, namely the Shiba multiplicative ansatz, and the so-called virtual-crystal off-diagonal CPA (VCA). These methods lead to worse and worse results, when the alloy parameters deviate from the restricted areas of their validity.

II. GENERALIZED BLACKMAN-ESTERLING-BERK FORMALISM

A. LCAO and the BEB formalism

This subsection and all of Sec. II are based on Ref. I, which attempts to apply systematically the LCAO representation to an *ab initio* description of random alloys. There are several requirements for such a theory to be met. First, it should be charge self-consistent based on spin-density-functional theory (SDFT). Second, the Kohn-Sham orbitals should be expanded to a sufficient degree of accuracy in a local orbital basis, consisting of a restricted set of ''atomic orbitals'' (AO's) and associated with each site. These orbitals may be selected as reasonably compressed quasiatomic wave functions, thus eliminating the unphysical effects of the tails of true atomic states, as described in Ref. 11 in the crystal case. The third natural requirement on a valid alloy theory is just that it should be an extension of a theory for perfectly periodic crystals. Such a philosophy had been behind an early attempt to develop an LCAO-CPA theory.[12] This precursor of Ref. I suffered from several limitations. It was not really charge self-consistent and the off-diagonal disorder was treated by averaging the random matrix elements (VCA CPA). Only the system chosen for application, the CuNi alloy, permitted limited success of the work. However, several important ideas, described below, have been suggested already there. Let us summarize the physical picture of a random alloy in the LCAO representation as it emerges from the analysis given in Ref. I.

(i) The atomic orbital set of a site must depend on its occupancy by a randomly selected atom, and thus it must be random itself. This permits to reproduce the random fluctuations in the charge density and in the orbital amplitudes, using an orbital set of a small dimensionality (usually just the minimum orbital set). As a consequence, the Hilbert space, spanned by the assembly of all AO, is itself random and depends on the *alloy configuration*, i.e., the random distribution of atoms of different sorts over the atomic sites. It becomes evident immediately that averaging over these alloy configurations in real space is unphysical and mathematically

difficult to understand. The configuration averaging is to be transferred to the matrix representation of the problem.

(ii) In principle, the matrix elements, involving the effective one-electron potential, depend on the total alloy configuration. It is natural to introduce an additional approximation, stating that the site diagonal elements depend only on the occupancy of the site, while the off-diagonal elements depend on the atomic occupancy of the two sites the orbitals are centered at (*terminal point approximation*). While this could be simply assumed, it is important to note that one of the main results of Ref. I represents an analysis of the random charge-density distribution and of the resulting one-electron potential, which indicates that the terminal point approximation is valid up to higher-order corrections. These are of about the same degree of importance and basically of the same origin as the corrections to the atomic sphere approximation in real-space theories of the KKR type.

(iii) This conclusion depends critically on the range of the AO used, which specifies also the range of nonzero matrix elements and thus the degree to which they will sample the environment of a given site. In the alloy case, it thus appears that the AO's should be even more compact than in case of crystals.

(iv) The requirement that the orbitals are compact in real space prompts them to be nonorthogonal between different sites; orthogonalization always leads to the occurence of orbital tails. The atomic orbital representation of the Kohn-Sham equations in this nonorthogonal basis thus leads to an algebraic problem, involving not only the Hamiltonian matrix but an overlap matrix as well. It is obvious that, in general, both the diagonal and the off-diagonal elements of these matrices will depend on the orbital site occupancy and thus they will be random. The off-diagonal randomness is then a natural companion of any atomic orbital theory of alloys.

(v) One of the crucial points for the proper description of random alloys is the identification of quantities that are subject to configuration averaging.[10] While it is obvious that all one-electron properties for a given alloy configuration are contained in the corresponding unaveraged Green's function, the object to be averaged is not the GF itself or its matrix representation but the observable quantities given by an (energy-dependent) functional $\mathrm{Tr}(AG)$ of the one-electron observables A. Even if A itself was nonrandom, its representation in the random AO basis becomes a random matrix. The configuration average of the trace then does not reduce to $\mathrm{Tr}(A\langle G\rangle)$, but can be shown to involve precisely the doubly conditional averages $G_{QQ'}$, mentioned in the Introduction and defined formally in the next subsection.

(vi) As has been established in Ref. I, this type of reasoning is essential for a charge self-consistent orbital theory in the single-site approximation. In the self-consistency loop, we may start from the random SDFT potential in real space. This is represented algebraically as a random matrix in the terminal point approximation. The corresponding matrix resolvent undergoes averaging, the outcome of which should be the conditional averages $G_{QQ'}$. In this approximate treatment, these quantities are combined with the atomic orbitals, belonging to the respective atomic species to generate the electron charge density in the real space, which fluctuates from site to site depending on the occupancy, while the averaging acts to suppress the random environment effects, in agreement with the single-site nature of the averaging procedure. From this charge distribution, a new one-electron potential is generated, and the loop is closed.

To summarize this overview, it appears that the task of achieving simultaneously the charge self-consistency and the self-consistent approximation for the alloy configuration average can be accomplished using the LCAO representation by mapping repeatedly the full real-space problem on an algebraic structure suitable for the configuration average and then reconstructing the real-space quantities in an inverse mapping.

It is also apparent from this discussion that the *natural algebraic mapping of the alloy problem is the BEB transformation*, which is capable of treating the combined diagonal and off-diagonal disorder in a single-site approximation and which leads directly to the required conditionally averaged Green's functions.

From this, the BEB theory was established in Ref. I as a tool for realistic LCAO calculations. In fact, it is very likely a minimum tool because a satisfactory fit of the real alloy BEB Hamiltonians by a Shiba-factorized model seems nonexistent in general.

Clearly, the original BEB has to be extended by including more orbitals per site and more inequivalent sublattices, permitting a partial long-range order. On top of that, the formalism must incorporate necessarily the overlap matrix along with the Hamiltonian matrix, since the atomic orbital basis is nonorthogonal.

All of this can be achieved conveniently by using a systematic scattering picture, which is transparent and easily manageable.

B. LCAO-BEB equations

1. Pseudospins and local orbital representation

In this section we combine the pseudospin description with the orbital approach to the electronic structure theory of a substitutionally disordered solid with an underlying lattice. Essentially, this leads to a generalized BEB formulation of the scattering problem. We only focus on the algebraic and analytic aspects of the theory. The discussion, concerning the charge self-consistency, is reported in Ref. I.

Let a lattice site be denoted by the multiple index $i=\vec{R}\vec{s}$, where $\vec{R}$ is a lattice vector and $\vec{s}$ is a basis vector within the unit cell. Let the lattice be occupied randomly with atoms of several species Q. The pseudospin is defined by

$$\eta^{Q}_{\vec{R}\vec{s}}=\begin{cases}1 & \text{atom of species } Q \text{ at } \vec{R}+\vec{s}\\ 0 & \text{otherwise,}\end{cases} \tag{1}$$

$$\sum_{Q}\eta^{Q}_{\vec{R}\vec{s}}=1.$$

One set of η's for all $\vec{R}\vec{s}$ and Q defines a configuration of the ensemble, describing a disordered solid. The consideration of a general unit cell with several basis vectors $\{\vec{s}\}$ includes the possibility of simulating long-range order via a sublattice dependent occupation probability:

$$\langle \eta^Q_{\vec{R}\vec{s}} \rangle = c^Q_{\vec{s}} \Rightarrow \sum_Q c^Q_{\vec{s}} = 1, \tag{2}$$

while requiring statistical independence of the pseudospins:

$$\langle \eta^Q_{\vec{R}\vec{s}}\ \eta^{Q'}_{\vec{R}'\vec{s}'} \rangle = c^Q_{\vec{s}} c^{Q'}_{\vec{s}'} \quad \text{for } \vec{R}+\vec{s} \neq \vec{R}'+\vec{s}'. \tag{3}$$

Now the basic concept of the orbital approach consists of expanding the one-electron wave function into a set of local overlapping AO's. For a disordered material, the contracted product of all possible AO's for all species with the pseudospin

$$|i\mu\rangle = \sum_Q |iQ\mu\rangle \eta^Q_i \tag{4}$$

selects the right orbital at the right site in a given configuration. The orbitals of neighboring sites are in general nonorthogonal, giving rise to an overlap matrix:

$$S_{ii',\mu\mu'} = \langle i\mu | i'\mu' \rangle = \sum_{QQ'} \eta^Q_i \langle iQ\mu | i'Q'\mu' \rangle \eta^{Q'}_{i'}. \tag{5}$$

The Hamiltonian represented by the AO's reads

$$H_{ii',\mu\mu'} = \langle i\mu | \hat{H} | i'\mu' \rangle = \sum_{QQ'} \eta^Q_i \langle iQ\mu | \hat{H} | i'Q'\mu' \rangle \eta^{Q'}_{i'}. \tag{6}$$

Now we expand the equation of motion for the retarded single-particle Greens's function in terms of those local orbitals:

$$(\omega^+ S - H) G^+ = 1, \tag{7}$$

where $\omega^+ = \omega + i0$, and G^+ is given in terms of the coordinates contragredient to Eq. (4):

$$G^+ = S^{-1} \langle\ |\hat{G}^+|\ \rangle S^{-1}. \tag{8}$$

The main η dependence of Eq. (6) is given by the dependencies at both terminal points. (A more complicated structure of H would result from core orthogonalization corrections and from third center potentials which, however, are self-averaging quantities.[1]) For the following we assume both the Hamiltonian and the overlap matrix to have a bilinear structure with respect to η

$$S = \eta^T \underline{S}\, \eta, \tag{9}$$

$$H = \eta^T \underline{H}\, \eta, \tag{10}$$

the meaning of which is the following: We introduced a compact method of notation of a matrix of the pseudospins $\eta = [(\delta_{ii',\mu\mu'} \eta^Q_i)]$ for a given ensemble configuration. Now H and S are matrices (with respect to site indices) of a given configuration, while $\underline{H} = [(H^{QQ'}_{ii,\mu\mu'})]$ and $\underline{S} = [(S^{QQ'}_{ii,\mu\mu'})]$ are matrices, acting in the expanded Hilbert space of the whole ensemble, which is provided with the full orbital basis. The pseudospins yield a connection between the operators of the ensemble with those describing a special configuration. The first kind of matrices (systematically denoted with an underbar) is translational invariant and nonstochastic while the second kind is stochastic and not translational invariant. If we deal with N basis orbitals in the crystal for each configuration and with M atomic species, then H is $N \times N$ and $\underline{H}$ is $MN \times MN$; η is $MN \times N$. These algebraic features are the prerequisites leading directly to a generalized BEB theory, applicable to nonorthogonal basis states and to complex substitutional disorder (sublattice dependent occupation probabilities).

2. Single-particle Green's function

Prepared with the algebraic representation of all matrices we now come to the formulation of the scattering problem for a substitutional disordered solid. From the pseudospins we may construct a stochastic projector, acting in the expanded Hilbert space:

$$\chi = \eta \eta^T, \quad \eta^T \chi = \eta^T, \quad \chi \eta = \eta\ . \tag{11}$$

This projector is a square diagonal matrix $\chi = [(\delta_{ii',\mu\mu'} \delta_{QQ'} \eta^Q_i)]$, obeying the relations

$$\chi^2 = \chi, \quad \mathrm{Tr}_Q \chi_{ii',\mu\mu'} = \delta_{ii',\mu\mu'}. \tag{12}$$

We can split the Hamiltonian and the overlap matrix into an on-site and an off-site part, where the on-site parts commute with the site-diagonal χ:

$$\underline{H} = \underline{\dot{H}} + \underline{\check{H}}, \tag{13}$$

$$\underline{S} = \underline{\dot{S}} + \underline{\check{S}}, \tag{14}$$

$$[\underline{\dot{S}}, \chi] = [\underline{\dot{H}}, \chi] = 0. \tag{15}$$

(The matrix $\dot{S}$ contains the orbital normalization, which may deviate from unity, e.g., by core orthogonalization corrections.) Inserting Eqs. (9),(10) into Eq. (7) we arrive at a Q-expanded equation of motion:

$$\eta^T (\omega \underline{S} - \underline{H})\, \eta G = 1. \tag{16}$$

Multiplying Eq. (16) with η on the left and with η^T on the right, we obtain an equation for the new quantity $\mathcal{G} = \eta G \eta^T$, representing the Green's function in the expanded Hilbert space, which, of course, depends on all pseudospins, that is, on χ:

$$\chi (\omega \underline{S} - \underline{H})\, \eta G \eta^T = \chi. \tag{17}$$

Now we use the properties of χ [Eq. (11)] and the commutation rules Eq. (15):

$$[\omega \underline{\dot{S}} - \underline{\dot{H}} + \chi (\omega \underline{\check{S}} - \underline{\check{H}}) \chi] \underline{\mathcal{G}} = \chi. \tag{18}$$

The expression on the left is Herglotz and thus can be inverted in the upper complex half plane:

$$\underline{\mathcal{G}} \equiv \eta G \eta^T = \chi \eta G \eta^T$$

$$= \chi[\omega \underline{\dot{S}} - \underline{\dot{H}} + \chi(\omega \underline{\check{S}} - \underline{\check{H}})\chi]^{-1}\chi \tag{19}$$

$$= \chi\Big[\underbrace{\omega \underline{\dot{S}} - \underline{\dot{H}} - \chi(\omega - \underline{\Sigma})\chi}_{\equiv -\underline{a}} + \chi \underbrace{\left(\omega - \underline{\Sigma} + \omega \underline{\check{S}} - \underline{\check{H}}\right)}_{\equiv \underline{\Gamma}^{-1}} \chi\Big]^{-1}\chi \,. \tag{20}$$

Here we introduced the complex self-energy Σ, the invertible scattering potential a and the coherent Green's matrix Γ. Now we use general rules for projectors to write

$$\underline{\mathcal{G}} = \chi(\chi \underline{\Gamma}^{-1}\chi - \underline{a})^{-1}\chi = \underbrace{-\chi \underline{a}^{-1}\chi}_{=\underline{b}}[\underline{\Gamma}^{-1}\chi \underline{a}^{-1}\chi - 1]^{-1}, \tag{21}$$

$$\underline{\mathcal{G}} = \underline{b}(\underline{b} - \underline{\Gamma})^{-1}\underline{\Gamma} = \underline{\Gamma} + \underline{\Gamma}(\underline{b} - \underline{\Gamma})^{-1}\underline{\Gamma} \equiv \underline{\Gamma} + \underline{\Gamma}\,\underline{T}\,\underline{\Gamma}. \tag{22}$$

Thus, we expressed the multiple scattering in terms of a coherent motion Γ and an incoherent stochastic part, the scattering matrix T. The CPA condition reads

$$\langle \underline{\mathcal{G}} \rangle = \underline{\Gamma} \quad \Leftarrow \quad \langle \underline{T} \rangle = \langle (\underline{b} - \underline{\Gamma})^{-1} \rangle \equiv 0. \tag{23}$$

This condition defines the self-energy Σ.

The charge density is needed for a charge self-consistent band-structure scheme. For this purpose the twofold conditional configurational averages of $\mathcal{G}$ are required. These quantities may be derived using projection properties of χ. From Eq. (19) we deduce

$$\underline{\mathcal{G}} = \chi \underline{\mathcal{G}} \chi, \quad \chi_{ii}^{QQ}|_{q \to i} = \delta_{qQ}, \tag{24}$$

$$\underline{\mathcal{G}}_{ii'}^{QQ'}\Big|_{\substack{q \to i \\ q' \to i'}} = \underline{\mathcal{G}}_{ii'}^{qq'}\Big|_{\substack{q \to i \\ q' \to i'}} \delta_{qQ,q'Q'}, \tag{25}$$

where the subscript $q \to i$ means to fix the species q at the site i. We sometimes use a block matrix notation and drop the subscripts $\mu\mu'$. The connection to the unconditionally averaged Greens' matrix Γ is given by

$$\Gamma_{ii}^{QQ'} = \langle \mathcal{G}_{ii}^{QQ'} \rangle = \sum_q c_i^q \langle \mathcal{G}_{ii}^{QQ'} \rangle_{q \to i} \delta_{Qq,Q'q}$$

$$= c_i^Q \langle \mathcal{G}_{ii}^{QQ} \rangle_{Q \to i} \delta_{QQ'} \tag{26}$$

and

$$\Gamma_{ii'}^{QQ'} = \langle \underline{\mathcal{G}}_{ii'}^{QQ'} \rangle = \sum_{qq'} c_i^q c_{i'}^{q'} \langle \underline{\mathcal{G}}_{ii'}^{QQ'} \rangle_{\substack{q \to i \\ q' \to i'}} \delta_{Qq,Q'q'}$$

$$= c_i^Q c_{i'}^{Q'} \langle \underline{\mathcal{G}}_{ii'}^{QQ'} \rangle_{\substack{Q \to i \\ Q' \to i'}}. \tag{27}$$

These equations define the twofold conditionally averaged Green's matrices. From the coherent Green's matrix we calculate the density of states:

$$\rho(\omega) = -\frac{1}{\pi}\mathrm{Im} \sum_{ii',QQ',\mu\mu'} S_{ii',\mu\mu'}^{QQ'} \underline{\Gamma}_{i'i,\mu'\mu}^{Q'Q} \tag{28}$$

and the Q-projected densities of states:

$$\rho^Q(\omega) = -\frac{1}{\pi}\mathrm{Im} \sum_{ii',Q',\mu\mu'} S_{ii',\mu\mu'}^{QQ'} \underline{\Gamma}_{i'i,\mu'\mu}^{Q'Q} \frac{1}{c_i^Q}. \tag{29}$$

Both expressions reduce to the normal trace in orthogonal basis schemes.

Up to this point, all formulas are exact on the basis of Eqs. (5) and (6). They provide an orbital representation of the multiple scattering theory in analogy to the KKR approach. For most practical calculations the CPA condition, Eq. (23), has to be simplified by using a single-site approximation. We neglect the site off-diagonal matrix elements of Σ. Then b becomes site diagonal and the scattering matrix T decouples:

$$\underline{T} = (1 - \underline{t}\,\underline{\Gamma}')^{-1}\underline{t}, \quad \underline{t}_{ii'} = \delta_{ii'}(\underline{b}_{ii} - \underline{\Gamma}_{ii})^{-1}, \tag{30}$$

$$\underline{\Gamma}'_{ii'} = (1 - \delta_{ii'})\underline{\Gamma}_{ii'}. \tag{31}$$

The CPA condition now reads

$$\langle \underline{t} \rangle \equiv 0. \tag{32}$$

For the conditional averaged Green's matrix we get the previous expressions:

$$\langle \mathcal{G}_{ii}^Q \rangle_{Q \to i} = \frac{\Gamma_{ii}^{QQ}}{c_i^Q}, \quad \langle \underline{\mathcal{G}}_{ii'}^{QQ'} \rangle_{\substack{Q \to i \\ Q' \to i'}} = \frac{\Gamma_{ii'}^{QQ'}}{c_i^Q c_{i'}^{Q'}}, \tag{33}$$

which are now correct, except for terms of the order $O(\langle \underline{t}^4 \rangle)$.

III. ANALYTIC PROPERTIES OF THE BEB THEORY

A. Limiting cases

Up to this point, we have introduced the generalized BEB theory and a single-site approximation for practical applications. The propagator formalism of Sec. II works in analogy to the original propagator formulation of the standard CPA. The main difference is the treatment of nonorthogonal basis sets, the inclusion of complex substitutional disorder (long-range order), and the BEB feature: diagonal and off-diagonal disorder of H and S are accounted for in the same manner.

In applying the CPA to band-structure calculations, it is important to know the accuracy with which this approximation treats the disorder problem. In the present section we will concentrate on the analytic properties of the generalized BEB theory.

As a first remark, we note that the BEB theory is equivalent to the original CPA if no off-diagonal disorder is present. This limit was already proved in the first BEB paper, Ref. 2. In the following discussion of the limiting behavior of BEB, there is thus at least one set of parameters that fulfills all discussed limits, since the original CPA does.

An important prerequisite to assure the physicality of the energy dependent quantities, like the self-energy and the Green's matrix, is the analyticity of these functions in the upper complex half-plane, the Herglotz property. It is met by the original CPA as well as by the Shiba transformation. Most of the attempts to construct a cluster CPA, first to generalize the CPA beyond the single-site level and second to include off-diagonal disorder, were suffering from nonanalyticities of some of the relevant functions. The inclusion of the off-diagonal disorder within the philosophy of single-site theories as done by BEB preserves the Herglotz property.[8]

The density of states of a tight-binding Hamiltonian is nonzero only within a certain energy range. The boundaries of this interval, the spectral bounds, are determined solely by the matrix elements of the Hamiltonian, see the Discussion in Sec. IV. These spectral bounds should be observed by any approximate alloy theory. At least, the density of states must not have any spectral weight outside of the spectral region. For the original CPA this was shown in Ref. 13 to be fulfilled. The structure of the BEB theory is mathematically more involved, and a proof for the correct limiting behavior has not been given. However, our numerical calculations have shown in no case a violation of the spectral bounds. The reproduction of all gaps, in contrast, is not possible with a single-site theory. Note, however, that the theorem, concerning the spectral bounds, does not yield any statement about the position of gaps, unless they are of split band nature, in which case the BEB CPA provides correctly the split band gap.

A seemingly crucial test of an alloy theory is the number of moments of the density of states that are reproduced correctly. This is due to the fact that the first few moments give some physically important information, such as the number of electrons, the band center, and widths. The BEB CPA gives correctly the first three moments of the spectral density and the first four moments of the total density of states (DOS).[2] This number is obviously smaller than in the original CPA. Nevertheless, the moment expansion of certain functions is known to converge extremely slowly. Thus, the number of preserved moments should be very large to assure the right shape of the density of states. Our numerical calculations show that, despite the poor number of preserved moments, the overall shape of the DOS is reproduced astonishingly well in BEB. Obviously, there is some other important information preserved in this theory, making it very appealing in real applications.

One major advantage of the original CPA was due to the fact that it provides an interpolation scheme between several limits known exactly in alloy theory. The first pair of limits concerns two extremal situations with respect to the scattering strength, that is, the weak-scattering limit and the split band limit. The latter occurs if the distance of the atomic levels by far exceeds the hopping integrals. The resulting DOS consists of two separated bands, reducing to the pure atomic level in cases, when the hopping integrals are approaching zero. This limit is discussed in Ref. 13. In the BEB theory the number of energy parameters is larger, thus, there are more possible limiting procedures. Blackman, Esterling, and Berk have given an analysis of the independent band limit, which sets in if the mixed hopping integral vanishes. Then no hopping between different species is possible and two independent bands should be expected. We again reach the split band limit in the sense discussed above by increasing now the distance between the atomic levels while keeping the hopping integrals constant. The opposite situation, having very small difference in the energy parameters, is called the weak-scattering limit. Here, the self-energy may be expanded with respect to the energy parameters around the virtual crystal approximation, say, the averaged Hamiltonian. Setting the off-diagonal hopping elements to the same value, we get the regime discussed in Ref. 13. Thus, the BEB theory provides an interpolation between the extreme situations with respect to the scattering parameters, similar to the original CPA.

The second pair of limits concerns the behavior with vanishing concentrations, called the dilute limit. First, one should note that the equations are symmetric with respect to an interchange of both species, thus, a subdivision into host species and impurity species is an arbitrary choice, as it should be. We will show that the BEB CPA becomes accurate in the dilute limit, for which—to the authors' best knowledge—no proof exists up to now in the literature. This dilute limit is not trivially fulfilled due to the concentrations in the denominator in Eq. (33).

B. Dilute limit

The generalized BEB CPA in the limit of vanishing concentration yields the single impurity Green's functions, for arbitrary off-diagonal matrix elements. The proof holds for nonorthogonal basis sets and for multiband cases as well.

1. Green's function of a general impurity

We start with deriving the Green's function for a single impurity. We consider a monoatomic lattice, occupied by the

sort A. In the origin we place an impurity atom B. The on-site elements $\dot{H}$ and the off-site elements $\check{H}$ of the Hamiltonian take the values

$$\dot{H}_{ii}=\begin{cases} V^A, & i\neq 0 \\ V^B, & i=0 \end{cases} \tag{34}$$

and

$$\check{H}_{ii'}=W_{ii'}^{QQ'}, \quad \left.\begin{matrix} Q \\ Q' \end{matrix}\right\}=A \quad \text{if} \quad \left.\begin{matrix} i \\ i' \end{matrix}\right\}\neq 0 \quad \text{and}$$

$$\left.\begin{matrix} Q \\ Q' \end{matrix}\right\}=B \quad \text{if} \quad \left.\begin{matrix} i \\ i' \end{matrix}\right\}=0. \tag{35}$$

The numbers $W_{ii'}^{QQ'}$ are not bound to the multiplicative condition $W_{ii'}^{QQ'}=\alpha^Q W_{ii'}\alpha^{Q'}$, used in the Shiba transformation.

In the following, we will omit the site indices if their values are obvious from the context. To distinguish between the impurity site and the A sites, we introduce projectors $\mathcal{P}$ and $\mathcal{Q}$ in real space, with

$$\mathcal{P}_{ii'}=\delta_{i0}\delta_{ii'}, \quad \mathcal{Q}=1-\mathcal{P}. \tag{36}$$

Furthermore, we abbreviate $l_{ii'}^Q=(\omega-V^Q)\delta_{ii'}$. We are interested in the elements of the Green's matrix at the impurity site 0. Using the projectors we write

$$g_B\equiv\mathcal{P}[\omega-H]^{-1}\mathcal{P}, \quad \mathcal{P}(\omega-H)\mathcal{P}=l^B,$$

$$\mathcal{P}(\omega-H)\mathcal{Q}=\mathcal{P}W^{BA}\mathcal{Q}, \tag{37}$$

$$\mathcal{Q}(\omega-H)\mathcal{P}=\mathcal{Q}W^{AB}\mathcal{P}, \quad \mathcal{Q}(\omega-H)\mathcal{Q}=\mathcal{Q}(l^A-W^{AA})\mathcal{Q}. \tag{38}$$

For any matrix $A=\mathcal{P}A\mathcal{P}+\mathcal{P}A\mathcal{Q}+\mathcal{Q}A\mathcal{P}+\mathcal{Q}A\mathcal{Q}$ one can show

$$\mathcal{P}A^{-1}\mathcal{P}=\left[\mathcal{P}A\mathcal{P}-\mathcal{P}A\mathcal{Q}\frac{\mathcal{Q}}{\mathcal{Q}A\mathcal{Q}}\mathcal{Q}A\mathcal{P}\right]^{-1}. \tag{39}$$

Thus, g_B can be expressed in terms of the Green's matrix $G_A=[l^A-W^{AA}]^{-1}$ of a pure A-medium (where W^{AA} is also used for $i=0$, $i'=0$):

$$g_B=\left[l^B-\mathcal{P}W^{BA}\mathcal{Q}\frac{\mathcal{Q}}{\mathcal{Q}G_A^{-1}\mathcal{Q}}\mathcal{Q}W^{AB}\mathcal{P}\right]^{-1}. \tag{40}$$

Note that the only nonzero matrix elements in l^B are l_{00}^B.

Equation (40) contains a term that may be called an origin-avoiding propagator $G_\emptyset$. It describes the propagation in the A medium under the condition that the site 0 is excluded from the path:

$$G_\emptyset=\frac{\mathcal{Q}}{\mathcal{Q}G_A^{-1}\mathcal{Q}}. \tag{41}$$

Using a relation, obtained from Eq. (39) by exchanging $\mathcal{P}$ with $\mathcal{Q}$, we have

$$G_\emptyset=\mathcal{Q}\left[G_A-G_A\mathcal{P}\frac{\mathcal{P}}{g_A}\mathcal{P}G_A\right]\mathcal{Q} \tag{42}$$

with $g_A=\mathcal{P}G_A\mathcal{P}$. The result is origin-avoiding, since the inverse of $-g_A$ in Eq. (42) represents the single-site scattering matrix of an infinite energy barrier, eliminating the origin from the path. (See for instance Ref. 14.) Finally, we insert $G_\emptyset$ in Eq. (40) and use $\mathcal{P}\check{H}\mathcal{P}=0\rightarrow\mathcal{P}\check{H}\mathcal{Q}=\mathcal{P}\check{H}$:

$$g_B=\left[l^B-\mathcal{P}W^{BA}\mathcal{Q}\left(G_A-G_A\mathcal{P}\frac{\mathcal{P}}{g_A}\mathcal{P}G_A\right)\mathcal{Q}W^{AB}\mathcal{P}\right]^{-1}$$

$$=\left[l^B-\mathcal{P}W^{BA}\left(G_A-G_A\mathcal{P}\frac{\mathcal{P}}{g_A}\mathcal{P}G_A\right)W^{AB}\mathcal{P}\right]^{-1}, \tag{43}$$

$$g_B=\left[l^B-g_M+g_L\frac{1}{g_A}g_R\right]^{-1}. \tag{44}$$

Here, the definitions $g_M\equiv\mathcal{P}W^{BA}G_AW^{AB}\mathcal{P}$, $g_L\equiv\mathcal{P}W^{BA}G_A\mathcal{P}$, and $g_R\equiv\mathcal{P}G_AW^{AB}\mathcal{P}$, are introduced. Equation (44) is the Green's function of the impurity and gives the density of states of one B atom in the A medium.

Furthermore, the propagator from the B atom into the A medium is an interesting element of the Green's matrix. It can be calculated from $[\omega-H]^{-1}$ via a relation similar to Eq. (39):

$$G_{BA}=\mathcal{P}[\omega-H]^{-1}\mathcal{Q}=g_B\mathcal{P}W^{BA}\mathcal{Q}\frac{\mathcal{Q}}{\mathcal{Q}G_A^{-1}\mathcal{Q}},$$

$$G_{BA}=g_B\mathcal{P}W^{BA}\left[G_A-G_A\mathcal{P}\frac{\mathcal{P}}{g_A}\mathcal{P}G_A\right]\mathcal{Q}. \tag{45}$$

It is worth noting that all formulas in this section hold for the most general case of an impurity, which means that the hopping elements $\check{H}$ may take any value. The condition of multiplicative disorder is not required. (Note, however, that for nearest-neighbor hopping only, multiplicative disorder would not be a restriction in the present context, since W^{BB} does not figure here and can be put to any value.)

2. The dilute-limit in the BEB CPA

In Sec. II B 2 we generalized the BEB CPA on the basis of a pseudospin description. There were some peculiarities. First, some elements of the self-energy are known analytically for vanishing concentrations (Sec. III C). They give rise to undefined expressions in the formalism if the corresponding rows and columns are not removed from the very beginning. Second, the physically meaningful, component projected elements of the Green's matrix are given by Eq. (33) with the concentrations appearing in the denominator. Nevertheless, the system of equations for the determination of the physical Green's matrix is well defined. This will be shown in the present subsection.

We will restrict ourselves to the case of a binary completely disordered alloy. Without loss of generality we may set the overlap matrix S to unity in the present context.

We recall briefly the basic formulas. The components are A with concentration $y=c_A$ and B with concentration $x=1-y=c_B$. All entities of the BEB CPA are matrices in the expanded Hilbert space. The coherent Green's matrix is given by

$$\underline{\underline{\Gamma}}=[\omega-\underline{\underline{\Sigma}}-\underline{\underline{\check{H}}}]^{-1} \quad . \tag{46}$$

The self-energy $\underline{\underline{\Sigma}}$ is assumed to be site diagonal. With $\underline{\underline{l}}=\omega-\underline{\underline{\dot{H}}}$ and $\underline{\underline{\gamma}}\equiv\underline{\underline{\mathcal{P}}}\underline{\underline{\Gamma}}\underline{\underline{\mathcal{P}}}$ we may write

$$\underline{\underline{a}}=-\underline{\underline{l}}+\chi(\omega-\underline{\underline{\Sigma}})\chi, \tag{47}$$

$$\underline{\underline{b}}=\chi\underline{\underline{a}}^{-1}\chi, \tag{48}$$

$$\underline{\underline{t}}=[\underline{\underline{b}}-\underline{\underline{\gamma}}]^{-1}, \tag{49}$$

$$\langle\underline{\underline{t}}\rangle=0. \tag{50}$$

(Here, $\mathcal{P}$ is a projection to an arbitrary site. Since all sites are identical, $\mathcal{P}$ may be thought to project to the origin.) Together with the projection properties of the χ matrices implying

$$\underline{\underline{\gamma}}^{QQ'}\propto\delta_{QQ'}, \tag{51}$$

the set of equations of the BEB CPA is completely defined. The physical matrix elements $\langle\mathcal{G}_{ii}^{Q}\rangle_{Q\to i}$ and $\langle\mathcal{G}_{ii'}^{QQ'}\rangle_{\substack{Q\to i\\ Q'\to i'}}$ and hence the DOS are given by Eq. (33).

From the definition Eq. (34) the matrix elements of the matrix b for a special choice of the site occupation q are given by

$$\underline{\underline{b}}^{(q)QQ'}=\delta_{QQ',Qq}\frac{1}{V^{Q}-\underline{\underline{\Sigma}}^{QQ'}}. \tag{52}$$

(Site indices suppressed.) Thus $\underline{\underline{t}}$ takes the form

$$\underline{\underline{t}}^{(q)QQ'}=\delta_{QQ'}\left[\delta_{Qq}\left[\frac{1}{V^{Q}-\underline{\underline{\Sigma}}^{QQ'}}-\underline{\underline{\gamma}}^{Q}\right]^{-1}+(\delta_{Qq}-1)\frac{1}{\underline{\underline{\gamma}}^{Q'}}\right]. \tag{53}$$

From the CPA condition $\Sigma_q c^q \underline{\underline{t}}^{(q)QQ'}=0$ we get two equations:

$$\underline{\underline{\Sigma}}^{QQ}=V^{Q}-\frac{1-c^{Q}}{\underline{\underline{\gamma}}^{Q}}, \quad Q=A,B. \tag{54}$$

The remaining two conditions are fixed by Eq. (51). We insert the elements of the self-energy and the off-site elements of the Hamiltonian, Eq. (35), in Eq. (46):

$$(\underline{\underline{\Gamma}}^{-1})^{QQ'}=\left(\omega-V^{Q}+\frac{1-c^{Q}}{\underline{\underline{\gamma}}^{Q}}\right)\delta_{QQ'}-W^{QQ'}-\underline{\underline{\Sigma}}^{QQ'}(1-\delta_{QQ'}). \tag{55}$$

We will elucidate the 2×2-matrix structure of this supermatrix by writing $\underline{\underline{\Gamma}}$ as a 2×2 matrix, the elements of which are matrices in the real space:

$$\underline{\underline{\Gamma}}=\begin{pmatrix} G_A^{-1}+\dfrac{x}{\underline{\underline{\gamma}}^{A}} & -(\underline{\underline{\Sigma}}^{AB}+W^{AB}) \\ -(\underline{\underline{\Sigma}}^{BA}+W^{BA}) & G_B^{-1}+\dfrac{y}{\underline{\underline{\gamma}}^{B}} \end{pmatrix}^{-1} \quad . \tag{56}$$

$G_Q=(l^Q-W^{QQ})^{-1}$ denotes the Green's functions in the pure Q media. The inversion of the super matrix structure in Eq. (56) results in

$$\underline{\underline{\Gamma}}^{QQ}=\left[G_Q^{-1}+\frac{c^{\tilde{Q}}}{\underline{\underline{\gamma}}^{Q}}-(\underline{\underline{\Sigma}}^{Q\tilde{Q}}+W^{Q\tilde{Q}})\times\frac{1}{G_{\tilde{Q}}^{-1}+\dfrac{c^{Q}}{\underline{\underline{\gamma}}^{\tilde{Q}}}}(\underline{\underline{\Sigma}}^{\tilde{Q}Q}+W^{\tilde{Q}Q})\right]^{-1}, \tag{57}$$

$$\underline{\underline{\Gamma}}^{Q\tilde{Q}}=\left[-(\underline{\underline{\Sigma}}^{\tilde{Q}Q}+W^{\tilde{Q}Q})+\left(G_{\tilde{Q}}^{-1}+\frac{c^{Q}}{\underline{\underline{\gamma}}^{\tilde{Q}}}\right)\frac{1}{\underline{\underline{\Sigma}}^{Q\tilde{Q}}+W^{Q\tilde{Q}}}\times\left(G_Q^{-1}+\frac{c^{\tilde{Q}}}{\underline{\underline{\gamma}}^{Q}}\right)\right]^{-1}. \tag{58}$$

We used $\tilde{Q}$ as an abbreviation for the component complementary to Q. All self-consistency equations of the BEB CPA are now contained in

$$\underline{\underline{\mathcal{P}}}\underline{\underline{\Gamma}}[\underline{\underline{\gamma}}]\underline{\underline{\mathcal{P}}}\equiv\underline{\underline{\gamma}}. \tag{59}$$

Now, we expand Eqs. (57),(58) with respect to the impurity concentration $c^B=x$. We insert

$$\underline{\underline{\gamma}}^{Q}=\underline{\underline{\gamma}}_{(0)}^{Q}+x\underline{\underline{\gamma}}_{(1)}^{Q}+x^2\underline{\underline{\gamma}}_{(2)}^{Q}+O(x^3), \tag{60}$$

$$\underline{\underline{\Sigma}}^{Q\tilde{Q}}=\underline{\underline{\Sigma}}_{(0)}^{Q\tilde{Q}}+O(x) \tag{61}$$

in these equations. The zeroth order of the function $\underline{\underline{\Gamma}}^{BB}$ is

$$\underline{\underline{\Gamma}}_{(0)}^{BB}=[\underline{\underline{\gamma}}_{(0)}^{B}G_B^{-1}+1-\underline{\underline{\gamma}}_{(0)}^{B}(\underline{\underline{\Sigma}}_{(0)}^{BA}+W^{BA})\times G_A(\underline{\underline{\Sigma}}_{(0)}^{AB}+W^{AB})]^{-1}\underline{\underline{\gamma}}_{(0)}^{B}. \tag{62}$$

The requirement $\underline{\underline{\mathcal{P}}}\underline{\underline{\Gamma}}^{BB}\underline{\underline{\mathcal{P}}}\equiv\underline{\underline{\gamma}}^{B}$ allows the unique solution $\underline{\underline{\gamma}}_{(0)}^{B}=0$. Remembering the formulas for the physical Green's function in Eq. (33) we see that this solution circumvents a divergence.

Furthermore,we get

$$\underline{\underline{\Gamma}}_{(0)}^{AA}=\left[G_A^{-1}-(\underline{\underline{\Sigma}}_{(0)}^{AB}+W^{AB})\times\frac{1}{\underline{\underline{\gamma}}_{(0)}^{B}G_B^{-1}+1}\underline{\underline{\gamma}}_{(0)}^{B}(\underline{\underline{\Sigma}}_{(0)}^{BA}+W^{BA})\right]^{-1}=G_A, \tag{63}$$

which leads immediately to $\underline{\gamma}^{A}_{(0)}=g_A\equiv\mathcal{P}G_A\mathcal{P}$. The mixed elements are given to zeroth order by

$$\underline{\Gamma}^{BA}_{(0)}=\underline{\gamma}^{B}_{(0)}\Bigg[-(\underline{\Sigma}^{AB}_{(0)}+W^{AB})\underline{\gamma}^{B}_{(0)}+G_A^{-1}\frac{1}{\underline{\Sigma}^{BA}_{(0)}+W^{BA}}\times(G_B^{-1}\underline{\gamma}^{B}_{(0)}+1)\Bigg]^{-1}=0=\underline{\Gamma}^{AB}_{(0)} \tag{64}$$

and using $\underline{\gamma}^{B}_{(0)}=0$ to first order by

$$\underline{\Gamma}^{BA}_{(1)}=\underline{\gamma}^{B}_{(1)}\Bigg[G_A^{-1}\frac{1}{\underline{\Sigma}^{BA}_{(0)}+W^{BA}}\Bigg]^{-1}=\underline{\gamma}^{B}_{(1)}(\underline{\Sigma}^{BA}_{(0)}+W^{BA})G_A\,. \tag{65}$$

The self-consistency conditions Eqs. (59),(51) result in

$$0\equiv\underline{\gamma}^{B}_{(1)}\mathcal{P}(\underline{\Sigma}^{BA}_{(0)}+W^{BA})G_A\mathcal{P} \tag{66}$$

and analogously in

$$0\equiv\mathcal{P}G_A(\underline{\Sigma}^{AB}_{(0)}+W^{AB})\mathcal{P}\underline{\gamma}^{B}_{(1)}\,. \tag{67}$$

Thus we need one further equation to determine $\underline{\gamma}^{B}_{(1)}$. After inserting $\underline{\gamma}^{B}_{(0)}=0$ the first order of $\underline{\Gamma}^{BB}$ only leads to an identity:

$$\underline{\Gamma}^{BB}_{(1)}=\underline{\gamma}^{B}_{(1)}\equiv\mathcal{P}\underline{\Gamma}^{BB}_{(1)}\mathcal{P}. \tag{68}$$

A peculiarity of the BEB theory is the fact that the second order of $\underline{\Gamma}^{BB}$ under the condition (59) does not introduce new unknown quantities:

$$\underline{\Gamma}^{BB}_{(2)}=\underline{\gamma}^{B}_{(2)}+[1-\underline{\gamma}^{B}_{(1)}G_B^{-1}+\underline{\gamma}^{B}_{(1)}(\underline{\Sigma}^{BA}_{(0)}+W^{BA})\times G_A(\underline{\Sigma}^{AB}_{(0)}+W^{AB})]\underline{\gamma}^{B}_{(1)}\,. \tag{69}$$

Thus we get with $\underline{\gamma}^{B}_{(2)}\equiv\mathcal{P}\underline{\Gamma}^{BB}_{(2)}\mathcal{P}$ and with $\mathcal{P}G_B^{-1}\mathcal{P}=l^B$ (see the definition of $\underline{\check{H}}$) an equation for $\underline{\gamma}^{B}_{(1)}$:

$$\underline{\gamma}^{B}_{(1)}=[l^B-\mathcal{P}(\underline{\Sigma}^{BA}_{(0)}+W^{BA})G_A(\underline{\Sigma}^{AB}_{(0)}+W^{AB})\mathcal{P}]^{-1} \tag{70}$$

From Eqs. (66),(67), using the definitions of the last section, we obtain the zeroth-order self-energies

$$\underline{\Sigma}^{BA}_{(0)}=-\mathcal{P}W^{BA}G_A\mathcal{P}\frac{\mathcal{P}}{\mathcal{P}G_A\mathcal{P}}\equiv-g_L\frac{1}{g_A}, \tag{71}$$

$$\underline{\Sigma}^{AB}_{(0)}=-\frac{\mathcal{P}}{\mathcal{P}G_A\mathcal{P}}\mathcal{P}G_AW^{AB}\mathcal{P}\equiv-\frac{1}{g_A}g_R \tag{72}$$

and finally from Eq. (70),

$$\underline{\gamma}^{B}_{(1)}=\Bigg[l^B-g_M+g_L\frac{1}{g_A}g_R\Bigg]^{-1} \tag{73}$$

and from Eq. (65)

$$\mathcal{P}\underline{\Gamma}^{BA}_{(1)}\mathcal{Q}=\underline{\gamma}^{B}_{(1)}\mathcal{P}\Bigg(-g_L\frac{1}{g_A}+W^{BA}\Bigg)G_A\mathcal{Q} \tag{74}$$

$$=\underline{\gamma}^{B}_{(1)}\mathcal{P}W^{BA}\Bigg(-G_A\mathcal{P}\frac{\mathcal{P}}{g_A}\mathcal{P}G_A+G_A\Bigg)\mathcal{Q}. \tag{75}$$

All together, the coherent Green's matrix $\underline{\Gamma}$ fits in the following scheme:

$$\underline{\Gamma}_{ii'}=\delta_{ii'}\begin{pmatrix}O(1)&0\\0&O(x)\end{pmatrix}+(1-\delta_{ii'})\begin{pmatrix}O(1)&O(x)\\O(x)&O(x^2)\end{pmatrix}. \tag{76}$$

Thus, no divergence problems occur while calculating the physical Green's function in Eq. (33). The Green's functions in the dilute limit read now

$$g_B=\Bigg[l^B-g_M+g_L\frac{1}{g_A}g_R\Bigg]^{-1} \tag{77}$$

and

$$G_{BA}=g_B\mathcal{P}W^{BA}\Bigg(-G_A\mathcal{P}\frac{\mathcal{P}}{g_A}\mathcal{P}G_A+G_A\Bigg)\mathcal{Q}. \tag{78}$$

These are the same formulas as for a single impurity in Sec. III B 1. All derivations were made, observing the commutation rules for matrices. This assures the validity of the proof even for the multiband case. The inclusion of the overlap matrix is straightforward by replacing $\dot{H}$ with $\dot{H}-\dot{S}\omega$ and $\check{H}$ with $\check{H}-\check{S}\omega$. We proved that the BEB CPA yields the single impurity Green's functions in the case of vanishing concentrations.

C. Self-energy

In cases of partially disordered alloys, some elements of the self-energy are known analytically. A proof is given in Ref. I. We give here a short summary of these results.

We will keep the full CPA equations without approximation. Then, the self-energy is not diagonal in real space. In the case of partially disordered alloys, there are sites whose occupation is fixed. Now we are going to investigate elements of Σ with respect to those sites (we call the indices f). It turns out that these elements are given by the explicit expressions

$$\underline{\Sigma}_{if}=\delta_{if}(\omega(1-\underline{\dot{S}}_f)+\underline{\dot{H}}_f). \tag{79}$$

Because a thus vanishes in the case of fixed site occupation, we have to exclude these sites from the CPA equations (23), (32) by deleting the corresponding rows and columns.

This result is somewhat unexpected. The physical picture behind the CPA is to put a single impurity atom in a lattice of the effective medium and to require that the averaged scattering at this impurity atom should vanish. This impurity atom is a local perturbation in the original CPA. However, in BEB theory this no longer holds, since here a coupling self-energy between different species exists. This self-energy indeed is local but the structure of the equations is different compared to the original CPA. The meaning of both self-energies is different. If transforming the BEB equations to a form comparable to the simple CPA equations, $\Sigma_{ii}^{QQ'}$ would transform into a nonlocal self-energy expression in the origi-

nal sense. This, finally, leads to the conclusion that the self-energy in BEB is extended over the whole lattice. [See the coupling of the self-energy to the off diagonal Hamiltonian elements in Eq. (57).]

Having this in mind, the result shown in this section is surprising. Even if the sublattices are coupled, the BEB self-energy between the sublattices will vanish for zero disorder at one site. The effective self-energy in the above-discussed sense, however, is not zero. The matrix structure of BEB is responsible for those properties. The mapping of disorder effects to the self-energy is well chosen. Obviously, disorder effects appear only in those matrix elements corresponding to disordered sites. Altogether, this is an indication for the BEB theory to be an extension of the CPA, going far beyond what is seen directly in comparing the equations. The local BEB self-energy has indeed a nontrivial nonlocal meaning.

This general peculiarity of Σ is preserved in the single-site approximation, where we set by definition all site off-diagonal elements of Σ to zero. Thus, it is clear that the BEB CPA will be the better, the less stochastic sites do exist in the unit cell. That provides us with an especially good justification of the single-site approximation in such cases. On the other hand, this feature allows us to reduce drastically the calculation time. The CPA equations for the fixed sublattices need not be solved numerically.

D. Comparison with other CPA extensions

We briefly summarize some other approaches to extend the original CPA. There is, first, the special case of the BEB theory, when the matrix elements fulfill the condition of multiplicative disorder, treated by the Shiba transformation. This method, based on a similarity transformation, maps the problem onto the original single-site CPA. It has obviously, all of the analytical features of the CPA. However, in general, the Hamiltonian, obtained by a LCAO method, and the corresponding overlap matrix never do fit simultaneously this multiplicative condition. In TB LMTO this special form is given automatically by the TB transformation, thus Shiba CPA is the appropriate tool for describing alloys in TB LMTO.

Besides the BEB and Shiba methods there are a couple of cluster CPA's to incorporate not only the off-diagonal disorder but also the disorder effects on the neighbor atoms. These methods suffer in general from two disadvantages. First, the Herglotz condition is violated in some of those theories, making the physical meaning dubious. However, the traveling cluster approximation[15,16] and the augmented space method of Mookerjee[17,18] appeared to be free of such problems and represent a reasonable generalization beyond the single-site level. The second, may be more important point is the enormous numerical effort, implied by the circumstance that the matrices, describing clusters of atoms, are now larger by an order of magnitude. This is especially troublesome for applications to more complex lattices. There is at least one quite simple cluster extension, the molecular cluster CPA, which unfortunately lowers the translational symmetry of the underlying lattice by grouping the atoms in a lattice of larger molecular clusters, thus increasing effectively the lattice constant. A survey of these methods is found in Ref. 19.

The form of the BEB Hamiltonian is still not the most general one. It is possible to construct more complicated dependencies of the matrix elements on the stochastic occupation of the neighbors. Those models are discussed, e.g., in Ref. 20. The special form of the BEB Hamiltonian was called in that work a canonical random operator. However, it was pointed out in Ref. I that the canonical form of the matrices appeared to be a direct consequence of the orbital approach.

IV. NUMERICAL TESTS OF BEB THEORY

A. Model Hamiltonian

In the preceding sections we introduced a version of the BEB-CPA generalized to nonorthogonal basis sets and to complex, sublattice-dependent substitutional disorder. The main progress of BEB, in comparison with the original CPA, is the proper treatment of the off-diagonal disorder. With the help of the powerful tool of projection techniques we have shown that the BEB CPA fulfills some rules, giving the hope, that it will be fortunate in band-structure schemes. Here we focus on a numerical test of the BEB CPA, both for complete and for partial disorder. This will also illustrate the analytical results of the preceding sections. We will compare components of the Green's matrix, calculated by the CPA with those given by direct simulation of an ensemble. Such numerical tests for the classical CPA were performed, i.e., by Ref. 21 or may be found in Refs. 14 and 19, but they were never done to our knowledge for the BEB theory.

We restrict ourselves to one-dimensional chains of atoms, well knowing that this type of model reveals some peculiarities, that are not as pronounced in higher-dimensional lattices. The effects, shown here, are common to all dimensionalities but are best seen in one-dimensional models. The canonical random tight-binding Hamiltonian of the chain has the form

$$\hat{H}=\sum_{iQ}\varepsilon_i^Q\eta_i^Q a_i^\dagger a_i+\sum_{i\neq i',QQ'}\eta_i^Q t_{ii'}^{QQ'}\eta_{i'}^{Q'}a_i^\dagger a_{i'}. \quad (80)$$

The overlap matrix is not considered here and hence set to unity. Equation (80) forms a one-band single-electron model with on-site energies ε_i^Q and with hopping integrals $t_{ii'}^{QQ'}$. The selection of the actual kind of atom at the position i is chosen by the pseudospin η_i^Q. All derivations of the last sections apply to this model. It is general enough not only to test the original BEB CPA but also the Shiba transformation, the VCA CPA and partially disordered chains.

With one exception we will consider in the following nearest-neighbor hopping only. All chains contain two kinds of atoms (A and B) with the energy parameters

$$\varepsilon^A\equiv 0,\quad \varepsilon^B,\quad t^{AA}\equiv 1,\quad t^{AB}=t^{BA},\quad t^{BB}. \quad (81)$$

The occupation probability of a sublattice site with the atom A is denoted by x, while the probability of B at the same site is denoted by $y=1-x$. They should be allowed to take site specific values, to simulate partial disorder (e.g., $x=0$ is possible). For this model we will calculate the density of states given by

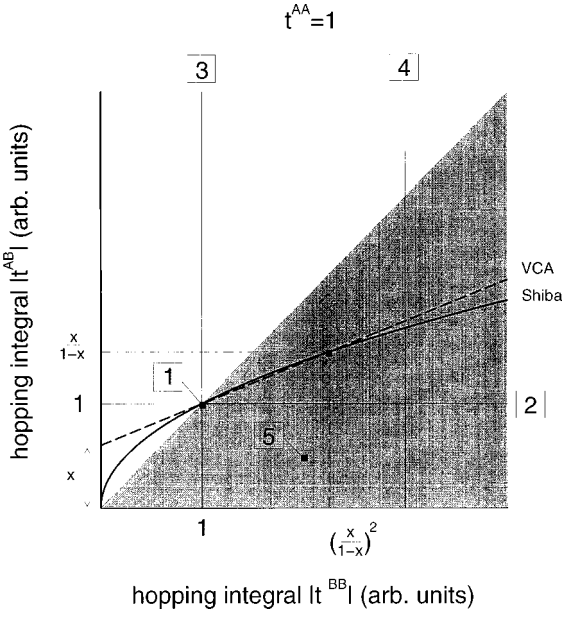

FIG. 1. Sketch of the parameter space of the binary -*X*- chain.

$$\rho(\omega) = -\frac{1}{\pi}\,\mathrm{Im}\,\mathrm{Tr}\,\underline{\Gamma}(\omega). \tag{82}$$

We computed the k-dependent Hamiltonian matrix and solved the BEB equations for a number of energy points. The mesh of k points was refined to obtain convergence of the density of states with respect to visible changes in the figures below. We chose 600 energy points in the depicted intervals. In order to get converged calculations, one has to obey the retardation condition by adding a small imaginary part to the energy; here we take the 1.5-fold of one energy step. This small imaginary part δ goes to zero with decreasing energy steps. Since the number of k-points depends on the smallness of δ, we are restricted to a certain choice. Nevertheless, the pictures do not change further with refinement of the mesh. The effect of broadening of the band edges, due to finite δ, is discussed below.

For the sake of comparison we will perform ''exact'' numerical simulations. We create an ensemble of stochastic configurations with specified energy parameters, Eq. (81), and specified concentrations with a sufficiently large number of members and build the Hamiltonian, corresponding to Eq. (80). Each member of the ensemble represents a chain of 300 sites with periodic boundary conditions. This length of the chains turned out to be large enough to give converged results. The random occupations of the sites were generated in a way to assure the right number of A and B atoms corresponding to the desired concentrations. That means, every member of the ensemble contains exactly the same number of atoms of the considered species. Since the DOS is self-averaging, a set of 200 configurations per ensemble turned out to be enough to obtain converged results. For each chain of the ensemble we diagonalized the Hamiltonian and calculated the density of states via

$$\rho(\omega) = -\frac{1}{\pi}\,\mathrm{Im}\sum_l \frac{1}{\omega + i\delta - \varepsilon_l}, \tag{83}$$

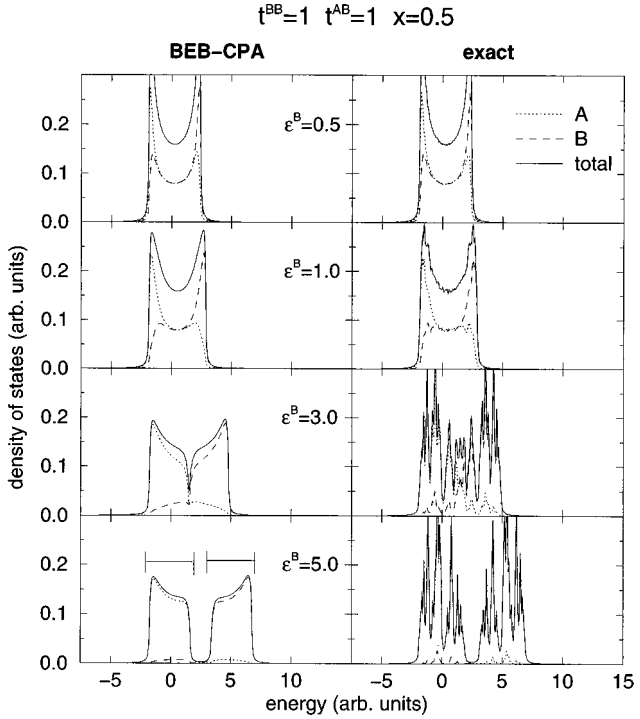

FIG. 2. DOS for a binary -*X*-*X*-*X*- chain at $x=0.5$ with varying diagonal energy parameters.

where ε_l are the eigenvalues of the Hamiltonian. Finally, the results for the ensemble were obtained by averaging the DOS over the set of configurations. As in the CPA calculations, we used 600 points along the energy axis in the shown intervals. The imaginary part δ of the energy ω was chosen again to be 1.5-fold of an energy step. This should assure the comparability of both results.

B. Binary model alloys

At the beginning we test completely disordered binary tight-binding chains of the shape -*X*-*X*-*X*- ($X=A,B$).

Figure 1 serves as a guide through the parameter space of the considered chain. It shows a sketch of the relevant region with respect to varying t^{AB} and t^{BB}. The numbers refer to the next five cases discussed below. From physical arguments one would expect, that the mixed hopping integrals are less than or equal to the pure hopping integrals. The shaded region represents these most probable sets of hopping integrals. It is worth noting that the hopping integrals, steaming form an LCAO Hamiltonian, are given in terms of matrix elements between local orbitals. Thus, their sign depends on the choice of phase factors. This leads to a unitary transformation describing the symmetry with respect to the phase changes. Fortunately, the BEB equations have this symmetry, thus, the choice of the phases of the orbitals is not significant.

Later on, we will compare the BEB CPA with the VCA CPA and Shiba CPA. The VCA CPA is the original CPA calculation, performed with a special choice of the off-diagonal hopping energy, which is not different for different species. The dashed line represents the relation between the hopping energy for the case of the VCA where all hopping elements are approximated by $t^{AB}_{\mathrm{VCA}} = x t^{AA} + y t^{BB}$.

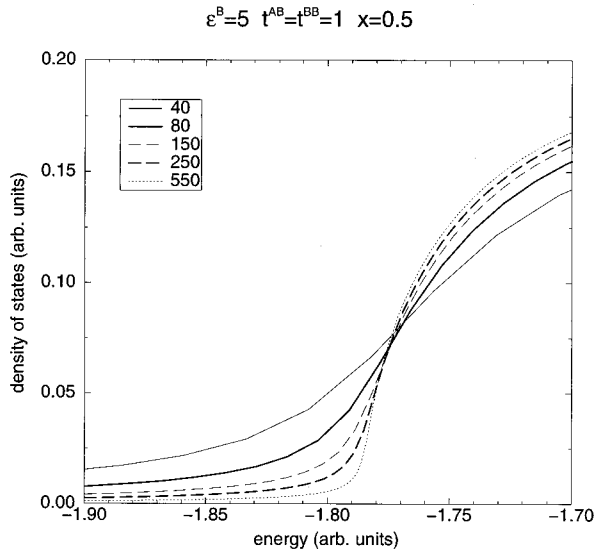

FIG. 3. Convergence of the band tails of the DOS towards the band edges for the -X- chain from Fig. 1 with increasing number of energy points per unit interval.

The Shiba CPA is characterized by the multiplicative condition for the values of the hopping integrals. For our purpose of testing the various CPA methods with respect to their applicability, in LCAO-CPA calculations we simulate a multiplicative fit of all Hamiltonian matrix elements by taking the geometric mean $t^{AB}_{\mathrm{Shiba}}=\sqrt{t^{AA}t^{BB}}$. The solid curve shows the connection of the hopping energies for this case. There are two points where both curves intersect, but only if all elements are unity both methods are equivalent.

The effects of disorder are most pronounced in concentrated alloys. Thus, we compare first the densities of states of the CPA and exact solution for $x=0.5$ in four rows in order to inspect the influence of the parameters ε^B, t^{BB}, and t^{AB}.

In Fig. 2 pure diagonal disorder is considered. All hopping integrals are set to unity. The only remaining parameter is the displacement of the band centers $\varepsilon^B-\varepsilon^A=\varepsilon^B$. It is called scattering strength. The partial and the total densities of states are shown. These partial densities of states are the concentration weighted, local, component-projected densities $-1/\pi\mathrm{Im}\Gamma^{QQ'}_{ii}(\omega)$. They give the energetic properties of a component Q, placed on a site i in an otherwise averaged crystal. For small diagonal disorder the CPA reproduces the DOS quite well. The shape is similar to the shape of the pure constituents bands with the bandwidth $W=4$ and square-root van-Hove singularities at the band edges. The only effect of disorder is a change in the band shape of the partial densities. With increasing scattering strength the split band regime sets in. Two subbands form, each of them lying in an energy region that is not occupied by states of the corresponding complementary pure component. Usually, such regions show peaks of local states. The CPA only gives bands there. They may be interpreted as arising from smearing out those peaks. By ε^B increasing to infinity, the ratio between the bandwidth of the split bands and their distance ε^B is decreasing. This results in two separate levels for $\varepsilon^B\rightarrow\infty$, called the split band limit. In this case the CPA turns out to become exact.[13]

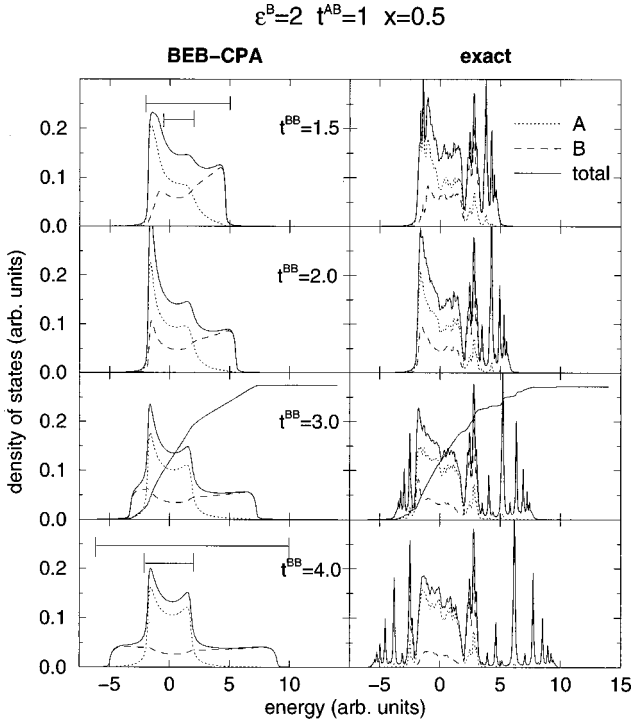

FIG. 4. DOS for a binary -X-X-X- chain at $x=0.5$ with varying B–off-diagonal energy parameters.

There are simple rules concerning the spectral region of tight-binding models.[22] The position of the energy levels and the hopping integrals to the nearest-neighbor sites of all possible local configurations determine the spectral region. For any arbitrary eigenvalue ω of the stochastic Hamiltonian, Eq. (80), there are one energy level $\varepsilon_i^{Q_i}$ and one constellation Q_i, $Q_{i'}$, which fulfill the condition

$$|\omega-\varepsilon_i^{Q_i}|\leqslant\sum_{i\neq i'}|t_{ii'}^{Q_iQ_{i'}}|. \tag{84}$$

We will call the ω region where each possible inequality of the above kind holds the main band. All regions outside of the main band possess more or less pronounced localized character: the spectral weight originate from clusters of the stronger scattering components. The union of all those intervals give the spectral bounds of the considered model Hamiltonian.

The two intervals, marked in the last panel of Fig. 2, give the spectral region, stated by this theorem, Eq. (84). An alloy theory must not give any spectral weight outside of this region. As is also seen in later figures, the BEB CPA does not violate this theorem. At the band edges the DOS has little tails reaching outside of the spectral intervals. This is due to the band broadening, induced by the finite imaginary part δ of the energy in those calculations. Figure 3 shows that, with increasing number of energy points per unit interval (and therefore with decreasing δ), these tails converge to the steep band edges.

In Fig. 4 the changes in the densities of states with varying bandwidth of the B component are shown for fixed diagonal disorder. It is an example for general off-diagonal disorder. The mixed hopping integral t^{AB} equals unity. That means, in each case, when a small connected cluster of B

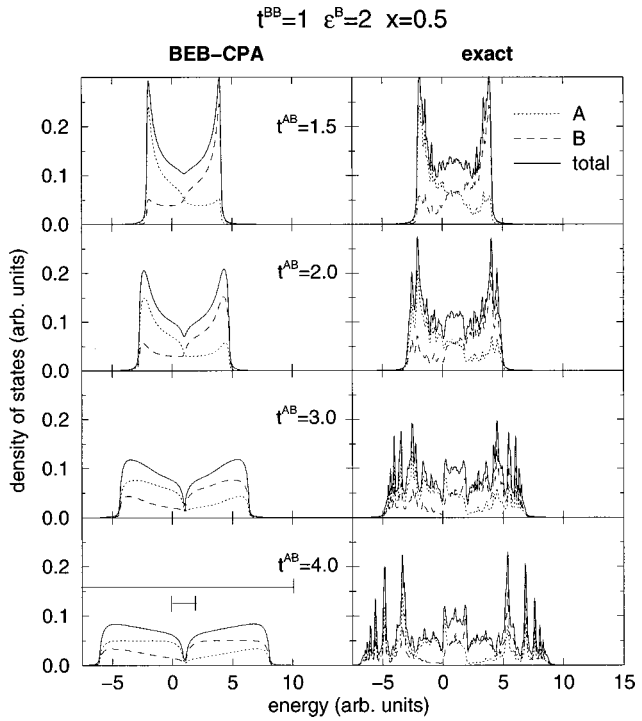

FIG. 5. DOS for a binary -X-X-X- chain at $x=0.5$ with varying mixed off-diagonal energy parameter.

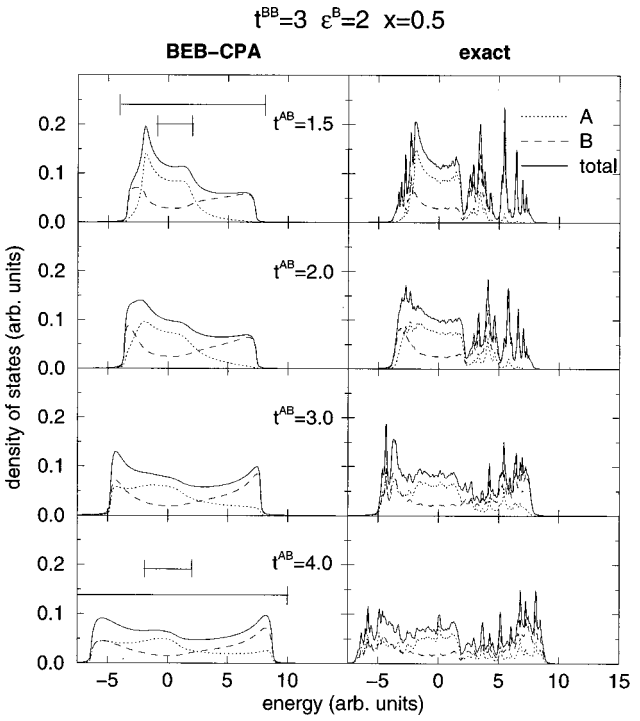

FIG. 6. DOS for a binary -X-X-X- chain at $x=0.5$ with varying mixed off-diagonal energy parameter.

atoms has formed, the hopping probability within this cluster is larger than the hopping out of it. This leads to an increased weight of the states lying outside of the pure A band, but inside the larger B band. Here, the BEB CPA provides similar but smoother shapes of the DOS within the main band, compared to the results of the simulations. In the region outside of the pure A band the BEB CPA broadens the large spectral peaks, while the rough shape is conserved. This is partially connected with the conservation of the first four moments of the density of states in the BEB CPA. Again, we marked the spectral regions in two panels. From now on, we always give two intervals. The shorter one is the region where all inequalities of Eq. (84) hold, the ''main band,'' while the longer interval is the union of all intervals, stated by the theorem: the maximum spectral region.

Additionally, we gave in one figure the integrated density of states (IDOS). (It saturates to unity, the scale is not given.) It is clearly seen that the overall shape of the IDOS is reproduced in BEB. Even in the spiky regions the exact IDOS fluctuates around the BEB result. Since the IDOS is the important quantity for real applications, this result is encouraging.

Now, we fix the hopping elements of the components A and B to unity and increase the mixed element t^{AB}. Then we obtain for $x=0.5$ pictures similar to the case of pure diagonal disorder, Fig. 5. For weak mixed disorder the BEB CPA describes the shape of the DOS quite well. If the disorder is increasing, extended regions of local states occur, which again are given by the CPA in a smeared out manner. The structure of the exact densities of states can be understood from considering the limiting cases. We restrict ourselves to the discussion of the case $t^{AB}=4$. Chains, consisting of pure components, form typical one-dimensional densities of states with bandwidth $W=4$, centered at $\varepsilon^A=0$ and $\varepsilon^B=2$. An ordered -A-B- chain possesses a gap in the energy interval $[0,2]$ and to the right and to the left of the gap it shows pronounced subbands. The statistical mixture of the components for $x=0.5$ creates large -A-B- chains as well as clusters of pure components. In the interval $[-2,2]$ the A-cluster states accumulate while in the interval $[0,4]$ the B-cluster states accumulate. In this special case the van Hove singu-

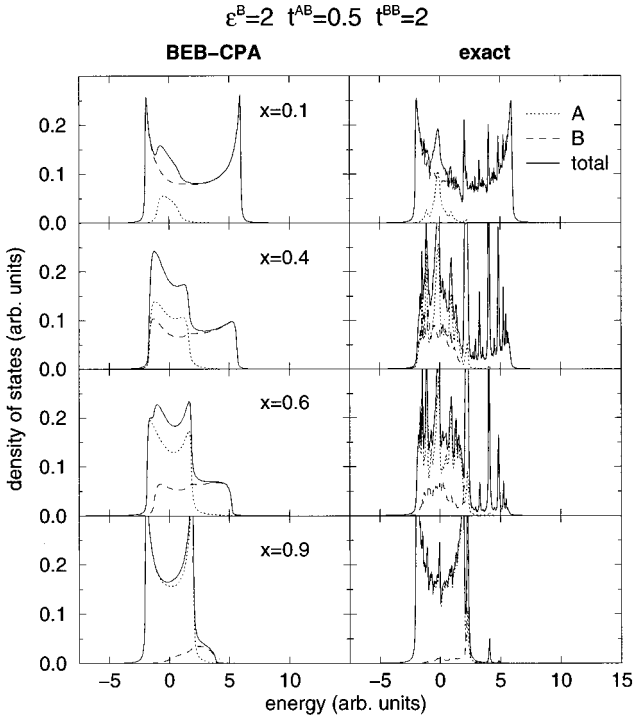

FIG. 7. DOS for a binary -X-X-X- chain with varying concentration for small mixed off-diagonal disorder.

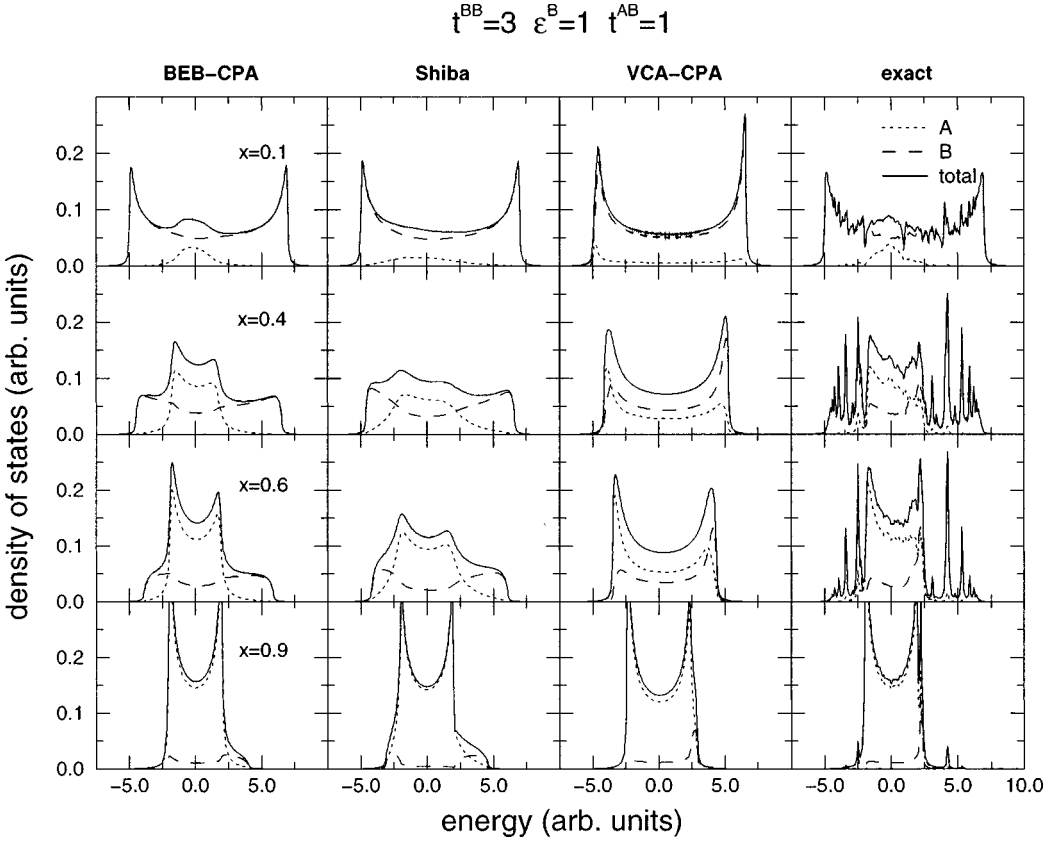

FIG. 8. DOS for a completely disordered binary chain at various concentrations: Comparison between the BEB CPA, Shiba CPA, and VCA CPA.

larities of the pure component DOS coincide even with the edges of the gap of the -*A*-*B*- chain. Both intervals of pure components overlap in the region [0,2]. This in consequence leads to an accumulation of states in this interval, in other words: the spectral weight in this region originates from cluster effects. The peaks outside of the elementary spectral intervals (-*A*- or -*B*- chains) have a strongly local character. The reasons are -*A*-*B*-*A*-*B*- clusters whose large hopping rate t^{AB} is favoring the trapping of an electron within the cluster. All the effects described above are strongly connected with a correlated occupation of neighboring sites. Surely, a single-site CPA never can account for this. Rather, it produces an interpolation between the densities of the pure chains. In the present case, the large t^{AB}, in connection with the neglect of cluster effects, yields a DOS, resembling that of the ordered -*A*-*B*- chain. The single-site CPA overemphasizes the alternating occurrence of the components. That means, in the region of the gap filled with cluster states in the exact solution, that the CPA supplies a low density of states. Nevertheless, the similarity of the smeared out CPA result with the exact DOS is seen at least for small t^{AB}. It should be clear from the above discussion that this set of parameters is quite critical for a single-site theory. Otherwise, this choice seems to be not quite physical.

If we now increase the hopping energy of the *B* atom while fixing a large t^{AB}, the strongly scattering -*A*-*B*- clusters are perturbed by -*A*-*A*- transitions only. Thus, the number of subchains with a large hopping rate is increasing and the gaps in the spectrum are filled. In Fig. 6 this behavior is shown for fixed *B* hopping t^{BB} and growing mixed hopping t^{AB}. The density of peaks is growing with increasing t^{AB}, since the number of energetically interrupted bonds is decreasing.

The strong broadening of the DOS with growing t^{AB} in Fig. 3 or the bandwidths in general can be understood with the help of the theorem Eq. (84).

A last example of this class of model chains is depicted in Fig. 5. Here, the mixed hopping is much smaller than the pure hopping elements. Again, the above statements hold. The shape of the BEB CPA is a smeared version of the spiky exact results. Note the resonance peak for $x=0.1$ which is reproduced quite well.

It becomes clear from Figs. 2, 4, and 5–7 that the BEB CPA yields reasonable results for moderately strong disorder if one accepts the broadening of spectral peaks in regions with strong localization character. We argue that this is not a critical point since many other reasons for broadening are not contained in our model. So, many-particle correlations would lead to a finite lifetime of all states.

Now, we turn to compare the BEB CPA with the Shiba CPA and with the VCA CPA, both being methods designed for the approximate treatment of off-diagonal disorder. For this we chose a chain with general (nonmultiplicative) off-diagonal disorder. Figure 8 shows the densities of states for these three methods together with the exact solutions with varying concentration. To apply the Shiba CPA to this model, it is necessary to perform the geometric average $t^{AB}_{\mathrm{Shiba}}=\sqrt{t^{AA}t^{BB}}=\sqrt{t^{BB}}$. For the VCA CPA we have to take the arithmetic mean $t^{AB}_{\mathrm{VCA}}=xt^{AA}+yt^{BB}$. The most important

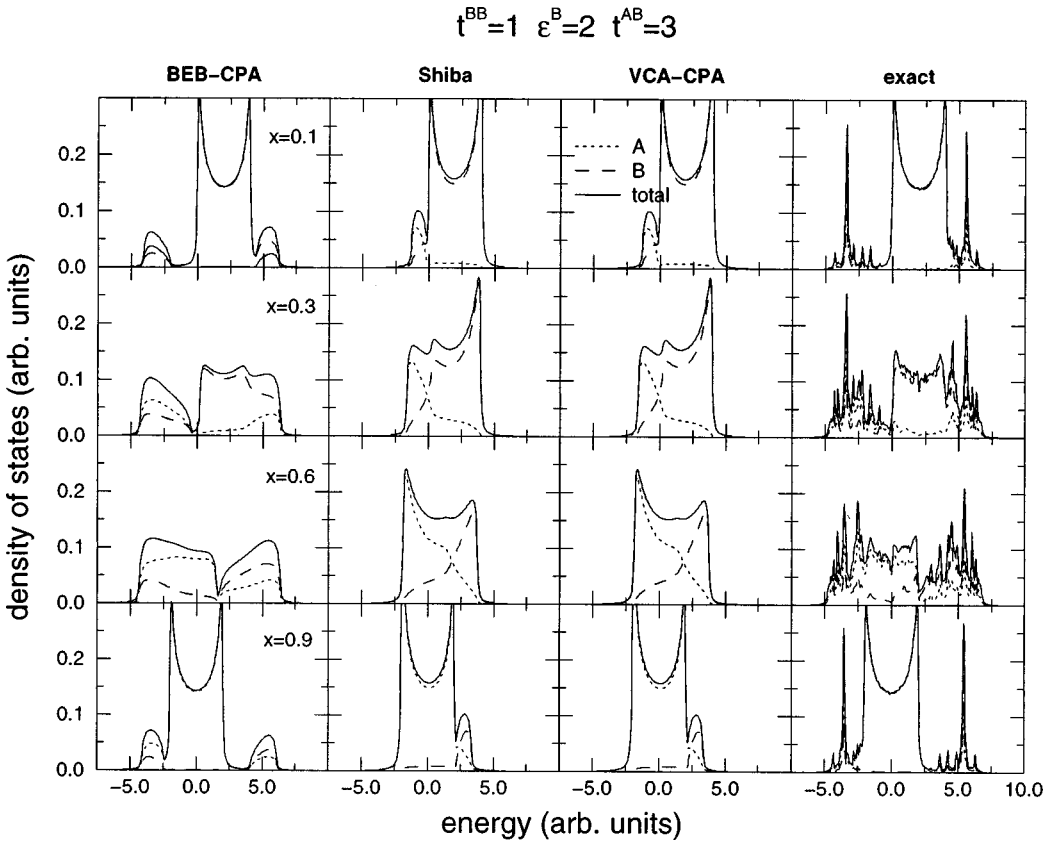

FIG. 9. DOS for a completely disordered binary chain with extreme mixed off-diagonal disorder at various concentrations: Comparison between the BEB CPA, Shiba CPA, and VCA CPA.

conclusion is that the off-diagonal disorder produces effects which can never be covered by a VCA CPA. The second conclusion is the observation that the Shiba transformation gives results similar to the BEB results for the actual parameter set. But only the BEB theory ensures that the first moments of the DOS are conserved. The shape of the Shiba DOS is similar by accident since the chosen $t^{AB}=1$ is close to the $t^{AB}_{\mathrm{Shiba}}=\sqrt{3}$. For other parameter sets, the shapes will be completely different, except for those that fulfill the multiplicative condition. A last statement concerns the low- and high-concentration case. Here, the BEB-CPA results are close to the exact ones, since BEB fulfills the single-impurity limit.

If the mixed hopping elements are larger than the pure hopping integrals, the Shiba CPA and VCA CPA start to fail completely even in predicting the bandwidths. Here, only the BEB CPA gives quite reasonable results. Such an extreme situation is drawn in Fig. 9. The pure hopping elements both are unity, thus $t^{AB}_{\mathrm{Shiba}}=t^{AB}_{\mathrm{VCA}}=1$ holds and the Shiba DOS and VCA DOS are identical. BEB again yields a broadened shape in regions of highly localized character. Even the -*A*-*B*–cluster peaks outside of the main band are reproduced approximately at low concentrations. The energy parameters are those from Fig. 3.

C. Partial disorder

This section is dedicated to partially disordered chains. As mentioned in Sec. III C the matrix elements of the self-energy between a site with fixed occupation and any other site is identically zero. Furthermore, the on-site elements of Σ at nonstochastic sites are known exactly and, therefore, they are included in the theory in a non approximate manner.

Hence, every nonstochastic site should improve the results of the generalized BEB CPA. We will see that this is

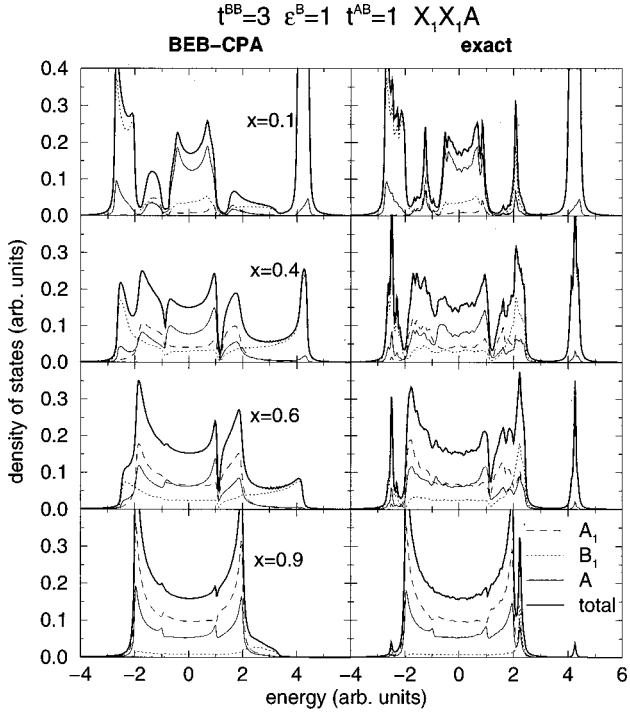

FIG. 10. DOS for a binary *X*-*X*-*A*- chain with partial disorder.

indeed the case, except for special parameter sets, which are critical especially in connection with the peculiarities of one-dimensional models.

In Fig. 10 we consider a chain, constructed from sequences -X-X-A. A denotes a site with fixed A occupation, while X denotes a stochastic place occupied by A with probability x and by B with probability y. The index 1 in the figure distinguishes the A atom at site X form the A atom at the fixed A site. It shows that both sites X have the same symmetry. The parameters are chosen to give a pure A band with bandwidth $W=4$ centered at $\varepsilon^A=0$. The B band has a bandwidth of $W=12$ and is centered at $\varepsilon^B=1$. The mixed hopping energy is unity and therefore lies within the energy regime of the pure A chain. This means that a B cluster is quite isolated energetically, since the high B-hopping rate favors a trapping of the electron within such a cluster. The arrangement of the components allows for B clusters with maximum length 2 only. This gives quite a large contribution from pair scattering events not contained in the single-site BEB. These strong correlations are especially important for concentrated alloys ($x\approx 0.5$). Even there, those pairs are present with large statistical weight. This lack of pair correlations is seen in the energy interval [2,4]. Here, the CPA closes a gap present in the exact solution. Obviously, the peak to the right is a B-B−cluster peak. Its height scales with the square of the probability y. Thus, the structure of the chain leads to strongly pronounced gaps, not described properly by a single-site CPA. Surely, the limiting cases of the pure A chain and the B-B-A chain are reproduced well.

Discussing the applicability of BEB CPA to realistic systems, it is worth noting that our one-dimensional models possess some peculiarities. First of all, every state is localized. Inevitably, each perturbation represents an obstacle for the propagation of excitations. In higher dimensions there are always paths avoiding the impurity for topological reasons. Therefore, the localization and cluster effects are less pronounced in higher-dimensional systems. Second, only the energy integral up to the Fermi energy of the Green's matrix is needed in charge self-consistent band-structure methods. Naturally, this quantity is much smoother than, for example, the density of states. Since, the BEB CPA yields smeared densities of states in the problematic energy regions, the shapes of which may be considered as average over the peaks, we would expect the BEB CPA to supply suitable expressions for an application in self-consistent calculations. Third, the tight-binding character of our model is very restrictive. We only allowed for nearest-neighbor hopping. Releasing this condition, the influence of an impurity is expected to be less dramatic. Figure 11 shows such an example. All parameters are identical with those in Fig. 10, except for the hopping integrals, which are changed according to

$$t_{ii'}^{QQ'}=t^{QQ'}e^{-\alpha(|i'-i|-1)} \tag{85}$$

with $t^{QQ'}$ taken from Eq. (81). That means, the nearest-neighbor hopping energies are the same. Additionally, we introduced exponentially decreasing hopping integrals to more distant sites. We chose $\alpha=1$, this corresponds to a reduction of the next-nearest-neighbor t compared to the nearest neighbor t by about 36%. This numerically small modification shows strong effects on the shape of the DOS. The reduced influence of impurities is seen clearly. It is interesting to note that the BEB results are almost identical to the numerical results. The contribution of the cluster peaks to the spectral weight is decreased or their width is broadened. We want to point out that the ansatz, Eq. (85), is not yet general enough, since the hopping energies for different distances are scaling with the same factor. This restriction may be raised. We also tested cases where the ratio t^{AA}/t^{BB} for next-nearest neighbors was inverted with respect to the ratio for nearest neighbors. Even in such extreme cases we could draw conclusions similar to the preceding ones.

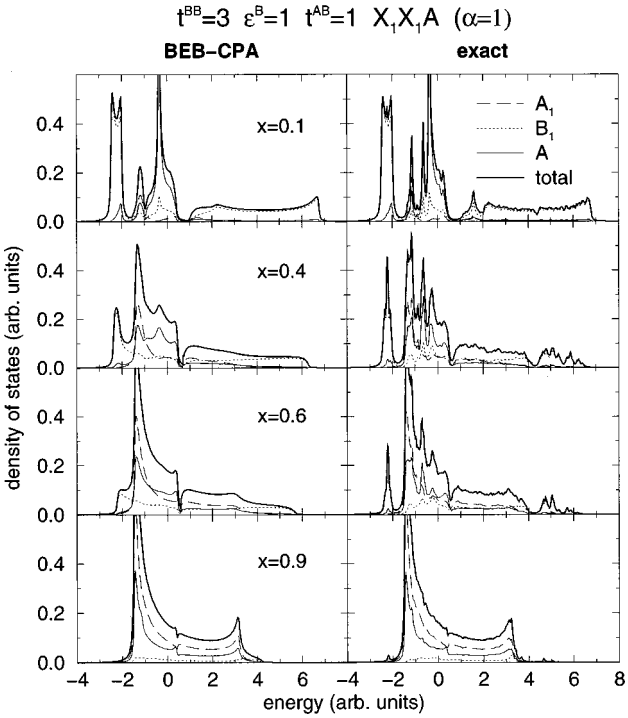

FIG. 11. DOS for a binary X-X-A- chain with partial disorder and more than nearest-neighbor hopping.

We want to present two further examples, including partial disorder to elucidate under which circumstances we may hope to obtain good results by applying the BEB CPA. The first chain has the unit cell -X-A-B-, Fig. 12. It is similar to the chain in Fig. 10. The limiting cases are the -A-A-B- and the B-A-B- chains. The latter one is identical with that of Fig. 10. Again, depending on the occupation of the site X, there are isolated B-B clusters. Nevertheless, the CPA result is now much better, since the correlation effects due to the B pairs are taken into account in a more accurate way by virtue of the properties of the self-energy. In particular, the self-energy at the fixed B site and all coupling elements between this site and any other are included in an exact way in the single-site BEB CPA. First approximations occur due to the neglect of the coupling between two stochastic sites X in different unit cells, separated by at least two sites. This coupling has not much influence on the DOS.

Figure 13 shows the chain -X-B-. The statistical occupation of a couple of neighboring unit cells with $X=B$ leads to large connected clusters of B atoms. Since the bandwidth of the pure B chain is much larger than that one of the A-B-chain, such clusters give rise to pronounced localization

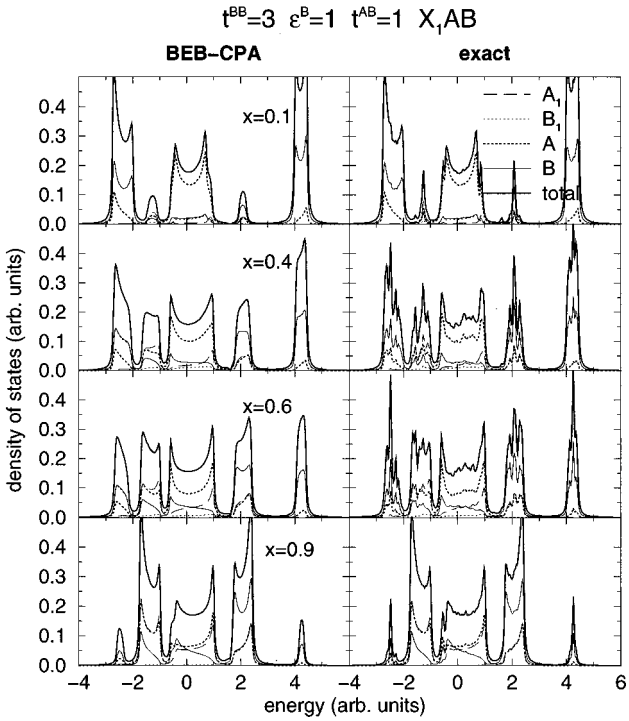

FIG. 12. DOS for a binary X-A-B- chain with partial disorder.

peaks outside of the main band. This effect again is given in the CPA by broadened and smooth curves.

D. Off-site elements of the Green's matrix

The last part of our inspection relates to a quantity, which to the authors' knowledge was not considered up to now in judging the quality of a CPA method. The most important questions while developing the CPA in earlier days were connected to the shape of the DOS. However, for the application to band-structure schemes with nonorthogonal basis sets, the off-site elements of the Green's matrix are as important as the on-site elements. Even the total charge is calculated, using the whole Green's matrix. We will examine some of those off-site matrix elements for two examples of disordered chains.

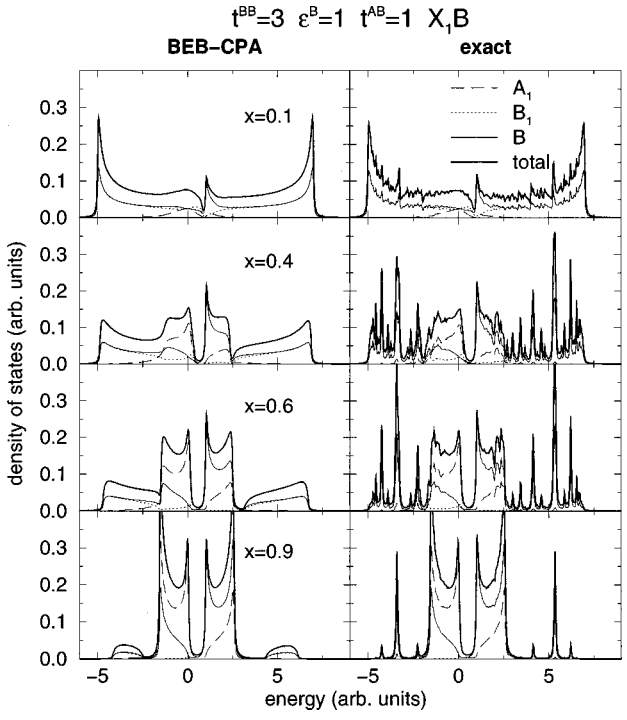

FIG. 13. DOS for a binary X-B- chain with partial disorder.

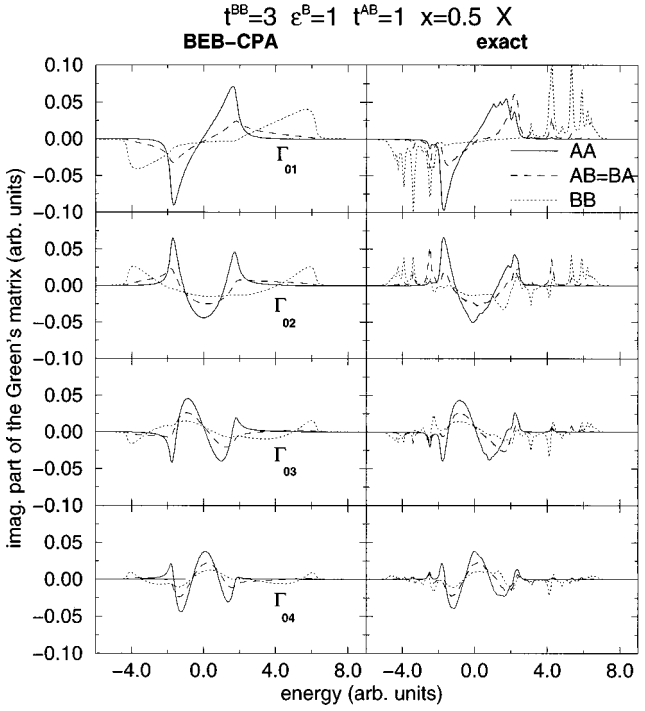

FIG. 14. Imaginary part of the energy-dependent off-site elements of the component projected Green's matrix for a completely disordered binary chain.

The first example is the completely disordered binary chain from Fig. 8. The energy parameters are taken from there and the concentration is set to $x=0.5$. (Here, we expect the largest effects of disorder.) Figure 14 shows the imaginary parts of the energy-dependent off-site elements of the Green's matrix:

$$-\frac{1}{\pi}\,\mathrm{Im}\,\Gamma^{QQ'}_{\substack{\vec{R}\vec{R}'\\ \vec{s}\vec{s}'}}(\omega), \tag{86}$$

denoted by $\Gamma_{\substack{RR'\\ ss'}}$ in the figure for simplicity. For the completely disordered case, the unit cell is simply -X-, hence $\vec{s}=\vec{s}'=0$ holds. The indices at Fig. 14 thus refer to the lattice sites $\vec{R}$, $\vec{R}'$. The different component-projected functions are marked. We see that the rough shape of the exact solution is reproduced by the CPA and that the deviations take place in the same energy regions as discussed for the DOS, namely, outside the main band. Furthermore, we see that the sign of the functions is essentially reproduced by the CPA. The smearing out is similar to the DOS case. All together, the off-site elements of the Green's matrix behave in the same way as the DOS.

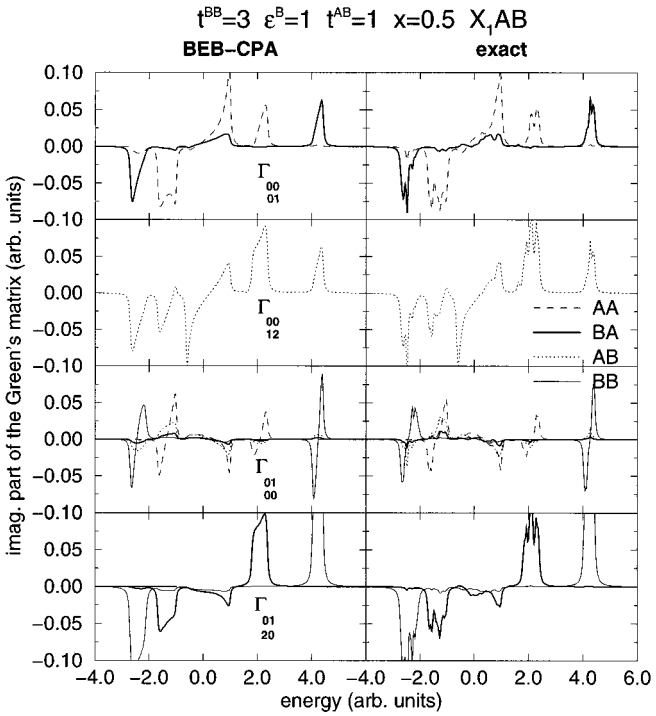

FIG. 15. Imaginary part of the energy-dependent off-site elements of the component projected Green's matrix for a partially disordered *X*-*A*-*B*- chain.

The second example corresponds to the partially disordered alloy in Fig. 12. The unit cell is -*X*-*A*-*B*-. Therefore, the indices $\vec{s}$ and $\vec{s}\,'$ may take the values 0, 1, and 2 for the sites *X*, *A*, and *B*, respectively. In Fig. 15 the indices relate to the indices at Γ in Eq. (86). Once again we show different component-projected functions, but not for all index combinations there are all variants. Here, in principle, the same statements hold as before. For this chain, the density of states was reproduced well by the CPA, now the same is true for the off-site elements. The energy regions, where deviations occur due to cluster peaks, are again the same either for the DOS or for the off-site elements. Thus, we expect the results and conclusions, obtained by analyzing the densities of states, to be applicable to the off-site elements of the Green's matrix, too.

V. CONCLUSION

We presented a generalized single-site CPA theory that is based on the concept introduced by Blackman, Esterling, and Berk. This theory is applicable to band-structure schemes, including nonorthogonal basis sets. Those orbital approaches to the density-functional theory naturally result in a structure of the Hamiltonian used in the BEB theory. Moreover, it is extended to complex disorder, including the possibility of simulating structural long-range order.

The outcome of the present work is a detailed inspection of some features of the BEB CPA. First, we developed the formalism within an orbital description of the scattering theory, the matrix form of which may be considered an analogy to the real-space theories (KKR). Then, we performed some analysis on the properties of the self-energy, holding in the single-site approximation as well as in the nonapproximate theory. These features give arguments in support of expecting the single-site BEB CPA to be a good approximation, particularly for partially disordered alloys. These analytic insights are further supported by the results obtained via numerical test in Sec. IV. The second analytic proof concerns the limit of small concentration. Here it turned out that the BEB CPA fulfills the condition to give the Green's function of a single impurity for vanishing concentration. This feature is fulfilled by the classical CPA and by the Shiba transformation (if the multiplicative condition for the off-diagonal disorder is appropriate). To the authors knowledge, this property was never proved before for the BEB CPA.

The last part of the present work gives an investigation of the range of parameters in which the CPA should be applicable. We think that the tests presented cover the essential patterns of behavior of the generalized BEB CPA, so that a generalization of the results is justified.

(i) It turned out that the CPA yields satisfactory results in a large parameter region of diagonal and off-diagonal disorder, respectively.

(ii) The statistical correlations between different sites give rise to peaks of local states, lying outside the main band. In these regions the single-site CPA supplies smeared out shapes of the DOS, which may be considered a reasonable smoothing of the exact DOS. This is supported by the statement that the first four moments of the DOS are conserved in the BEB theory.[2] Therefore, the energy integrated CPA-Green's matrix should give a suitable approximation to the exact one.

(iii) The observed deviations are expected to be smaller for realistic systems and higher dimensions.

(iv) For partially disordered systems, the results are usually quite good. The described exceptions are mainly connected to the special peculiarities of one-dimensional models with nearest-neighbor hopping only.

(v) Beside the on-site elements of the Green's matrix, the off-site elements were tested. They are needed in charge self-consistent bandstructure schemes, and therefore should be reproduced in equal accuracy. Our investigations assure that indeed off-site as well as on-site elements are given with the same quality.

All together, our inspection points out that the generalized BEB CPA represents a suitable and meaningful tool for the description of disordered and partially disordered alloys in the framework of band-structure schemes based on matrix formalisms.

ACKNOWLEDGMENTS

The authors acknowledge discussions with V. Drchal concerning the TB-LMTO CPA. Furthermore, we thank H. Fehske for useful hints related to the different types of off-diagonal disorder.

[1] K. Koepernik, B. Velický, R. Hayn, and H. Eschrig, Phys. Rev. B **55**, 5717 (1997).
[2] J. A. Blackman, D. M. Esterling, and N. F. Berk, Phys. Rev. B **4**, 2412 (1971).
[3] In *Methods of Electronic Structure Calculations*, edited by V. Kumar, O. K. Andersen, and A. Mookerjee (World Scientific, Singapore, 1992).
[4] D. M. Esterling, Phys. Rev. B **12**, 1596 (1975).
[5] H. Shiba, Prog. Theor. Phys. **46**, 77 (1971).
[6] J. A. Blackman, J. Phys. F **3**, L31 (1973).
[7] I. Turek, V. Drchal, J. Kudrnovský, and M. Šob, *Electronic Structure of Disordered Alloys, Surfaces and Interfaces* (Kluwer Academic, Boston, 1997).
[8] A. Gonis and J. W. Garland, Phys. Rev. B **16**, 1495 (1977).
[9] D. A. Papaconstantopoulos, A. Gonis, and P. M. Laufer, Phys. Rev. B **40**, 12 196 (1989).
[10] J. S. Faulkner and G. M. Stocks, Phys. Rev. B **21**, 3222 (1980).
[11] H. Eschrig, *Optimized LCAO Method and the Electronic Structure of Extended Systems* (Springer, Berlin, 1989).
[12] R. Richter, H. Eschrig, and B. Velický, J. Phys. F **17**, 351 (1987).
[13] B. Velický, S. Kirkpatrick, and H. Ehrenreich, Phys. Rev. **175**, 747 (1968).
[14] R. J. Elliott, J. A. Krumhansl, and P. L. Leath, Rev. Mod. Phys. **46**, 465 (1974).
[15] T. Kaplan, P. L. Leath, L. J. Gray, and H. W. Diehl, Phys. Rev. B **21**, 4230 (1980).
[16] R. Mills and P. Ratanavararaksa, Phys. Rev. B **18**, 5291 (1978).
[17] A. Mookerjee, J. Phys. C **6**, L205 (1973).
[18] A. Mookerjee, J. Phys. C **8**, 29 (1975).
[19] A. Gonis, *Green Functions for Ordered and Disordered Systems* (North- Holland, Amsterdam, 1992).
[20] K. Niizeki, Prog. Theor. Phys. **53**, 74 (1975).
[21] D. W. Taylor, Phys. Rev. **156**, 1017 (1967).
[22] J. M. Ziman, *Models of Disorder* (Cambridge University Press, London, 1979).